“Многокварковые конфигурации адронной материи в процессах с большими p_T. Часть1 Дикварки”

Шиманский С.С.

How many the diquark publications?

f t diquark and date < 2008 | Brief format | Искать | Easy Search | Расширенный поиск

find j "Phys.Rev.Lett.,105*" :: ещё

Сортировать по: earliest date | нисх. | - ИЛИ упорядочить по -

Представить результаты: 25 результаты | один список

673 записей найдено 1 - 25 перейти к записи: 1

f t diquark and date > 2007 | Brief format | Искать | Easy Search | Расширенный поиск

find j "Phys.Rev.Lett.,105*" :: ещё

Сортировать по: earliest date | нисх. | - ИЛИ упорядочить по -

Представить результаты: 25 результаты | один список

224 записей найдено 1 - 25 перейти к записи: 1

Transverse Momentum Distributions in Spin-1 Diquark Model
Navdeep Kaur, Narinder Kumar, Harleen Dahiya (Ambedkar, Nat. Inst. Technol.). 2018. 3 pp.
Published in Springer Proc.Phys. 203 (2018) 781-783

Parton distribution functions of proton in a light-front quark-diquark model
Tanmay Maji, Dipankar Chakrabarti (Indian Inst. Tech., Kanpur). Jan 5, 2018. 4 pp.
Published in Springer Proc.Phys. 203 (2018) 151-154

Spectroscopy of Exotic Hadrons Formed from Dynamical Diquarks
Richard F. Lebed (Arizona State U.). Sep 18, 2017. 14 pp.
Published in Phys.Rev. D96 (2017) no.11, 116003

Proton structure in a light-front quark-diquark model: Collins asymmetry
Tanmay Maji, Dipankar Chakrabarti (Indian Inst. Tech., Kanpur). Jan 5, 2018. 7 pp.
Published in PoS DIS2017 (2018) 193

Polarized heavy baryon production in quark-diquark model considering two different scenarios
S.Mohammad Moosavi Nejad (Yazd U. & IPM, Tehran), M. Delpasand (Yazd U.). 2017. 12 pp.
Published in Eur.Phys.J. A53 (2017) no.9, 174

Isospin breaking from diquark clustering
W.R. Gibbs (New Mexico State U.), Jean-Pierre Dedonder (Paris U., VI-VII). Jun 14, 2017. 19 pp.
Published in Phys.Rev. C96 (2017) no.3, 034001

Spin-1 diquark contributing to the formation of tetraquarks in light mesons
Hungchong Kim (Goyang, Korea Aerospace U.), Myung-Ki Cheoun (SoongSil U.), K.S. Kim (Goyang, Korea Aerospace U.). Nov 16, 2016. 9 pp.
Published in Eur.Phys.J. C77 (2017) no.3, 173, Erratum: Eur.Phys.J. C77 (2017) no.8, 545

An interacting quark-diquark model. Strange and nonstrange baryon spectroscopy and other observables
M. De Sanctis (Colombia, U. Natl.), J. Ferretti (INFN, Rome & Rome U.), R. Magaña Vsevolodovna, P. Saracco, E. Santopinto (INFN, Genoa). Aug 1, 2016. 8 pp.
Published in Few Body Syst. 57 (2016) no.12, 1177-1184

How Often Do Diquarks Form? A Very Simple Model
Richard F. Lebed (Arizona State U.). Jun 22, 2016. 7 pp.
Published in Phys.Rev. D94 (2016) no.3, 034039

Single Transverse Spin Asymmetries in Semi-inclusive Deep Inelastic Scattering in a Spin-1 Diquark Model
Narinder Kumar, Harleen Dahiya (Ambedkar, Nat. Inst. Technol.). Apr 15, 2015. 23 pp.
Published in Eur.Phys.J. A51 (2015) no.4, 51

Transverse polarization of the Λ hyperon from unpolarized quark fragmentation in the diquark model
Yongliang Yang, Zhun Lu (Southeast U., Nanjing), Ivan Schmidt (CCTVal, Valparaiso & Santa Maria U., Valparaiso). Jun 11, 2017. 10 pp.
Published in Phys.Rev. D96 (2017) no.3, 034010

Narrow pentaquarks as diquark-diquark-antiquark systems
V.V. Anisovich, M.A. Matveev (St. Petersburg, INP), J. Nyiri (Wigner RCP, Budapest), A.N. Semenova (St. Petersburg, INP). Jun 5, 2017. 7 pp.
Published in Mod.Phys.Lett. A32 (2017) no.29, 1750154

Searching for evidence of diquark states using lattice QCD simulations
Ryutaro Fukuda (RIKEN BNL & Tokyo U.), Philippe de Forcrand (CERN & ETH, Zurich (main)). 2017. 6 pp.
Published in PoS LATTICE2016 (2017) 121

From the inclusive experiments to the correlations and the exclusive experiments

"New directions in science are launched by new tools much more often than by new concepts.

The effect of a concept-driven revolution is to explain old things in new ways.

The effect of a tool-driven revolution is to discover new things that have to be explained"

From Freeman Dyson 'Imagined Worlds'

HESR - High Energy Storage Ring

- Production rate 2×10^{7}/sec
- P_{beam} = 1 - 15 GeV/c
- N_{stored} = 5×10^{10} $\bar{p}$
- Internal Target

$2.3 \le \sqrt{s} \le 5.5$ GeV

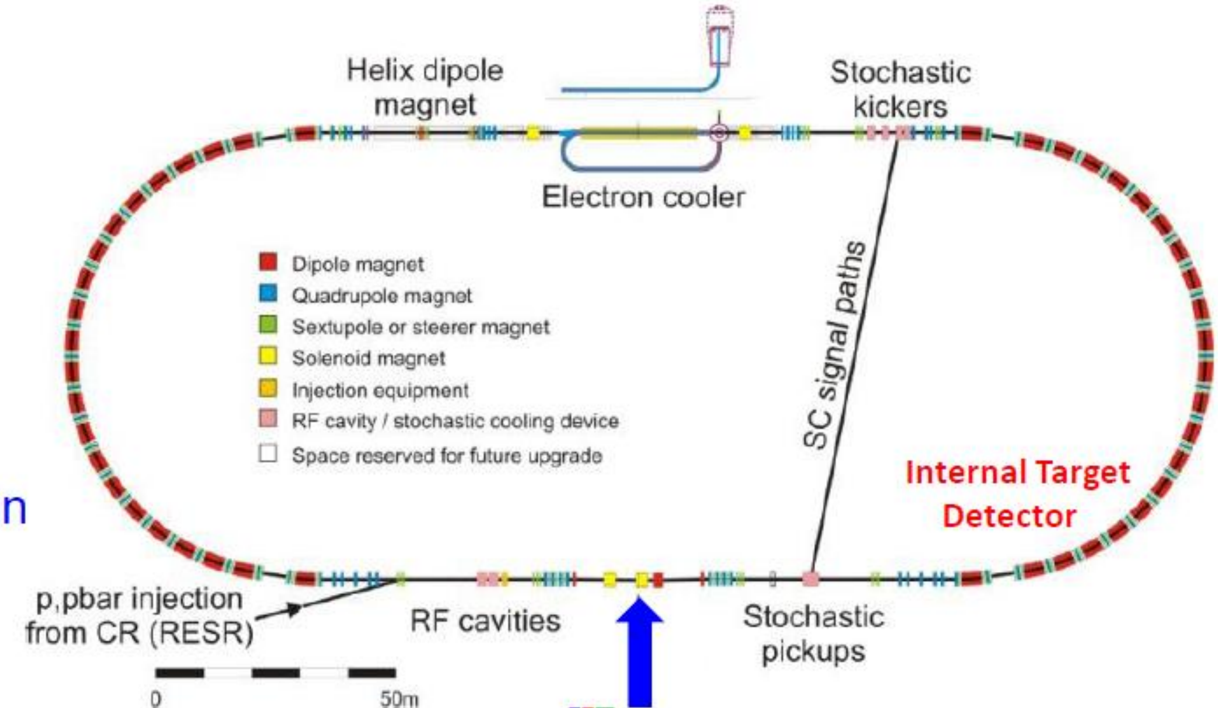

High resolution mode

- $\delta p/p \sim 10^{-5}$ (electron coolin
- Lumin. = 10^{31} cm^{-2} s^{-1}

High luminosity mode

- Lumin. = 2×10^{32} cm^{-2} s^{-1}
- $\delta p/p \sim 10^{-4}$ (stochastic cooling)

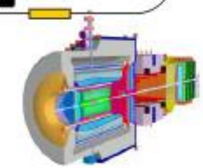

PANDA Spectrometer

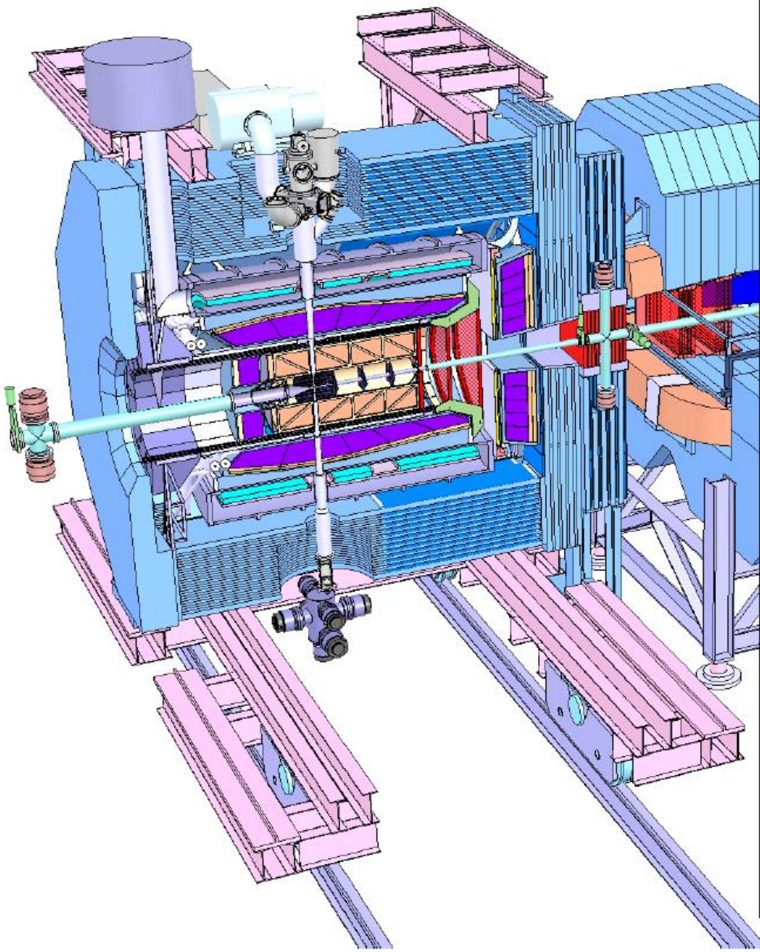

Detector requirements:

- 4π acceptance

- High rate capability: $2 \times 10^{7}\ s^{-1}$ interactions
- Efficient event selection

➔ *Continuous acquisition*

- Momentum resolution ~1%
- Vertex info for D, K^0_S, Υ ($c\tau$ = 317 μm for $D^{\pm}$)

➔ *Good tracking*

- Good PID (γ, e, μ, π, K, p)

➔ *Cherenkov, ToF, dE/dx*

- γ-detection MeV – 15 GeV

➔ *Crystal Calorimeter*

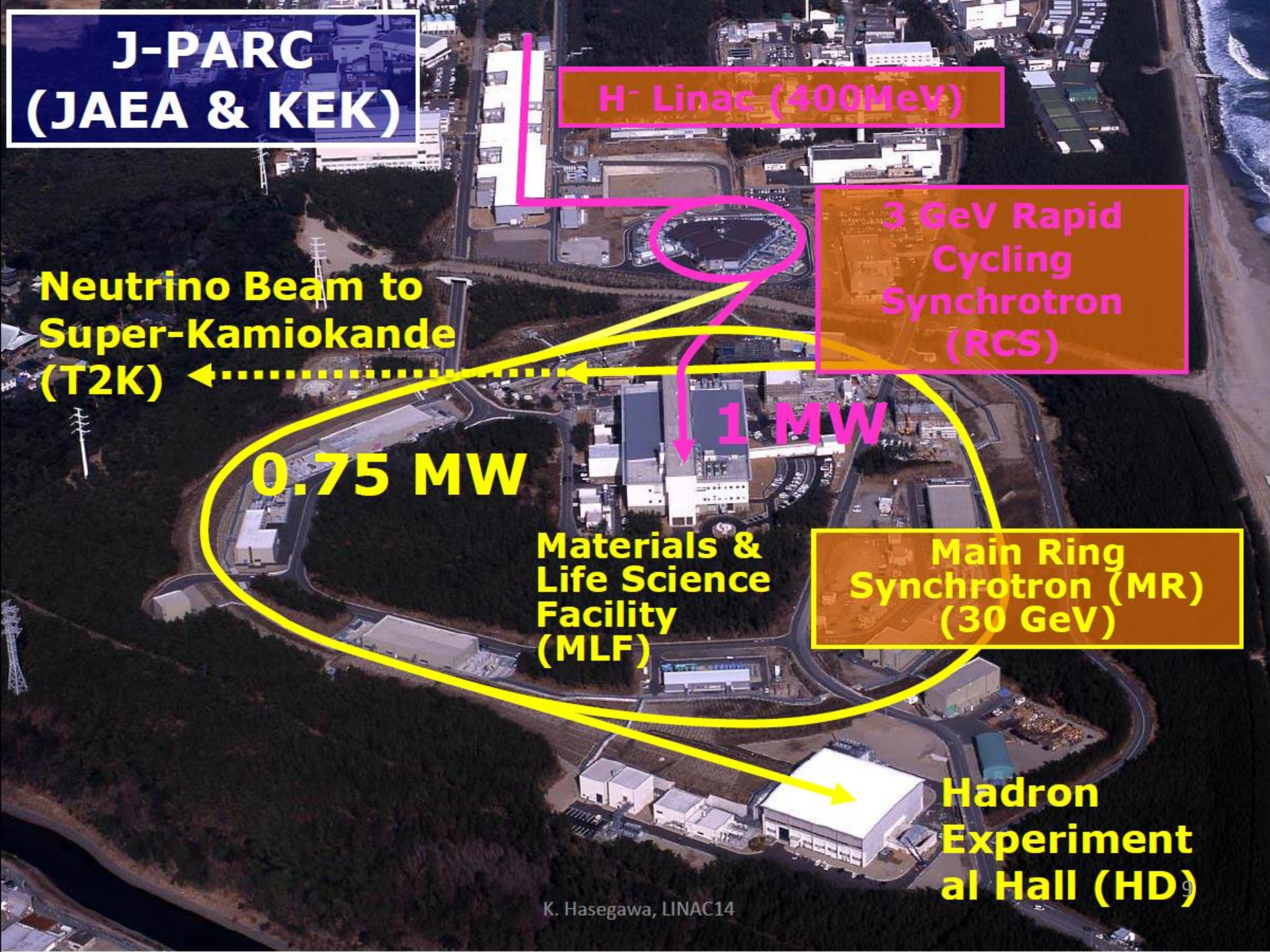
J-PARC
(JAEA & KEK)
H- Linac (400MeV)
3 GeV Rapid Cycling Synchrotron (RCS)
Neutrino Beam to Super-Kamiokande (T2K)
1 MW
0.75 MW
Materials & Life Science Facility (MLF)
Main Ring Synchrotron (MR) (30 GeV)
Hadron Experimental Hall (HD)

ELSEVIER

Available online at www.sciencedirect.com

ScienceDirect

Nuclear Physics A ••• (••••) •••–•••

NUCLEAR PHYSICS A

www.elsevier.com/locate/nuclphysa

2014

Towards the heavy-ion program at J-PARC

H. Sako [a,b,*], T. Chujo [c], T. Gunji [d], H. Harada [b], K. Imai [a], M. Kaneta [e], M. Kinsho [b], Y. Liu [f], S. Nagamiya [a,g,f], K. Nishio [a], K. Ozawa [f], P.K. Saha [b], T. Sakaguchi [h], S. Sato [a], J. Tamura [b]

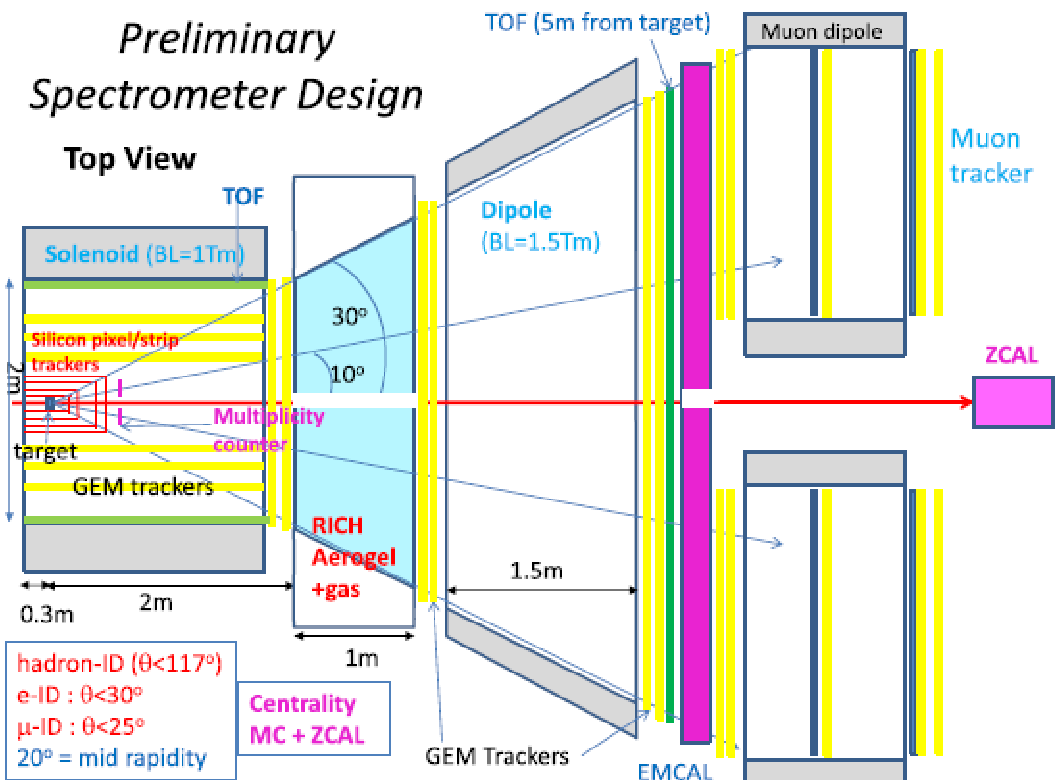

Fig. 2. A schematic view of the preliminary experimental setup.

Letter of Intent for J-PARC Heavy-Ion Program (J-PARC-HI)

J-PARC-HI Collaboration

Spokesperson H. Sako*[1,2],

July 25, 2016

2016

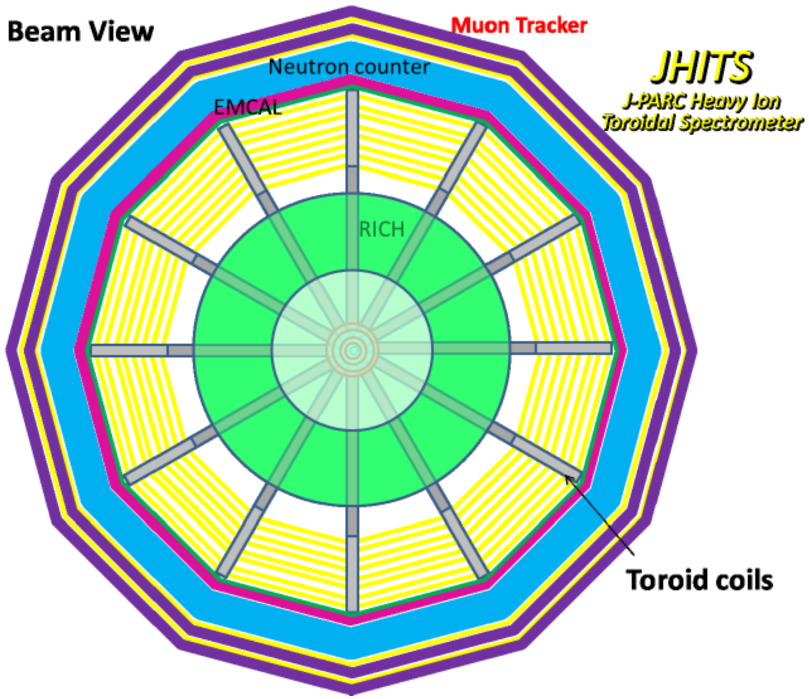

Beam View
Muon Tracker
Neutron counter
EMCAL
RICH
JHITS
J-PARC Heavy Ion
Toroidal Spectrometer
Toroid coils

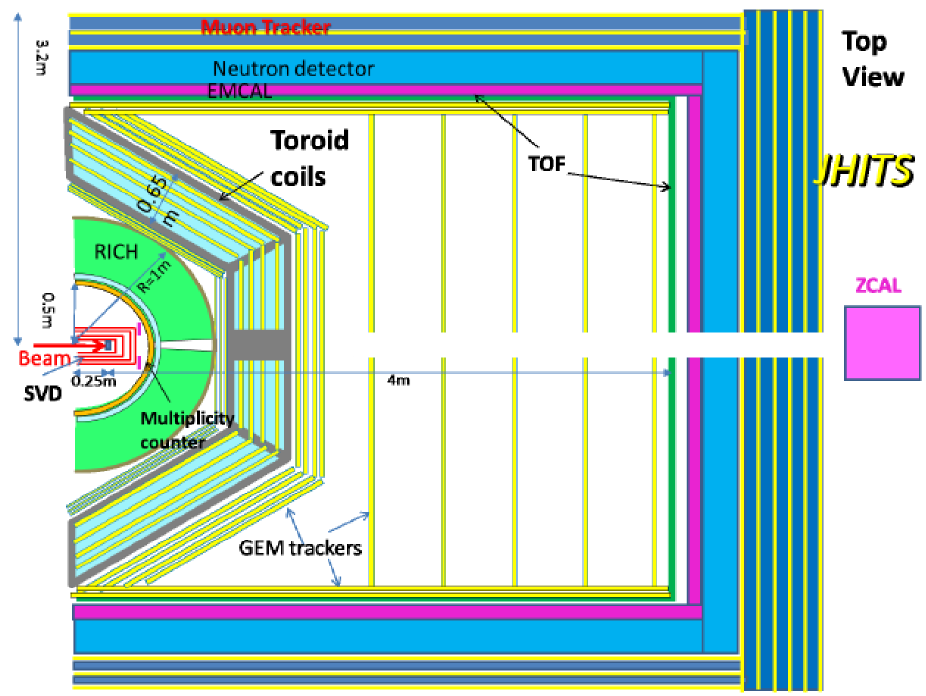

Muon Tracker
Neutron detector
EMCAL
3.2m
Toroid
coils
TOF
0.65
m
RICH
R=1m
0.5m
Beam
0.25m
SVD
4m
Multiplicity
counter
GEM trackers
Top
View
JHITS
ZCAL

Requirements for the SPD

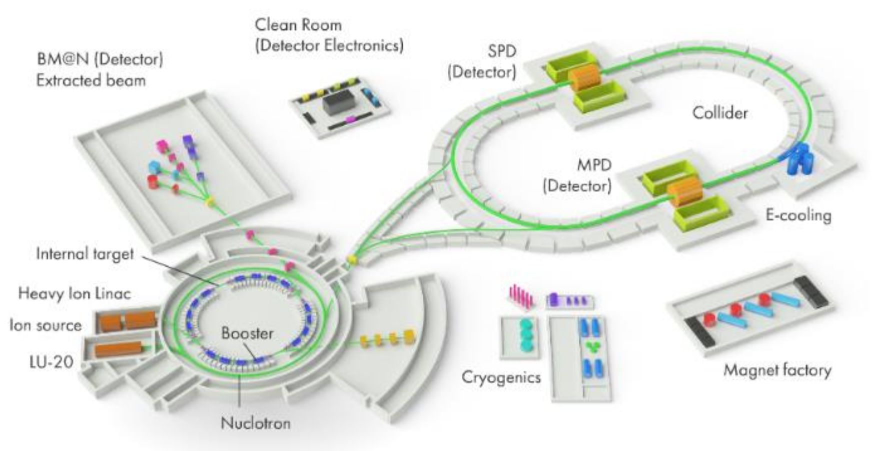

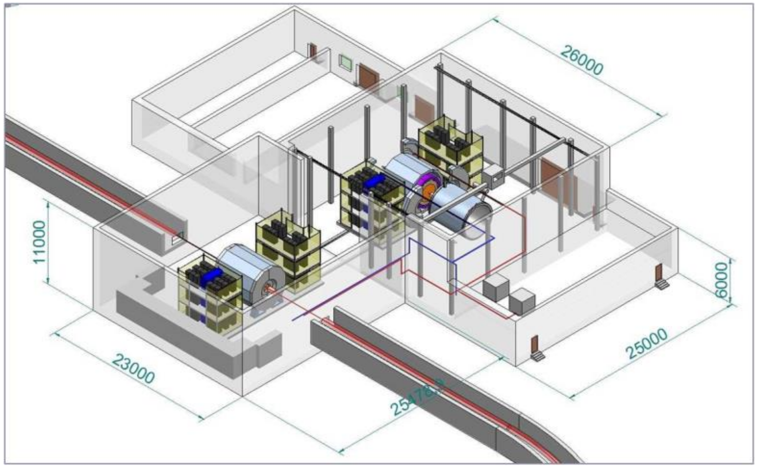

- close to 4π geometrical acceptance;
- high-precision (~50 µm) and fast vertex detector;
- high-precision (~100 µm) and fast tracker,
- good particle ID capabilities;
- efficient muon range system,
- good electromagnetic calorimeter,
- low material budget over the track paths,
- trigger and DAQ system able to cope with event rates at luminosity of 10^{32} $(cm.s)^{-1}$,
- modularity and easy access to the detector elements, that makes possible further reconfiguration and upgrade of the facility.

Main advantages

The unique beams: **– wide range of kind of the beam particles (antiproton and polarization) and $\Delta p/p$ up to 10^{-5}.**

The unique detectors: **$\Delta\Omega \sim 4\pi$ (exclusive reactions, correlations, backward range); detection all kinds of particles; working at luminosity ~ 10^{32} cm^{-2} s^{-1} (the rare event can be investigated); PID – close to full energy range and high momentum resolution.**

HIGH p_T ISSUES at SPD

1. Diquark properties.
2. Nature of the spin effects.
3. Exotic states and flavor universality.
4. FSI (with s,c-quarks participation).
5. ΛN - hypernuclei.

6. Nature of CsDBM.
7. Subthreshold J/Ψ production.
8. The Deuteron spin structure.
9. np dilepton production anomaly.
10. …

Why the high p_T is needed?

The Counting Rules

In 1973 were published two artiles :

Matveev V.A., Muradyan R.M., Tavkhelidze A.N. ***Lett. Nuovo Cimento 7,719 (1973);***

Brodsky S., Farrar G. ***Phys. Rev. Lett. 31,1153 (1973)***

Predictions that for momentum $p_{beam} \geq 5$ GeV/c in any binary large-angle scattering ($\theta_{cm} > 40°$) reaction at large momentum transfers $Q = \sqrt{-t}$:

$$A + B \to C + D$$

$$\frac{d\sigma}{dt}_{A+B\to C+D} \sim s^{-(n_A+n_B+n_C+n_D-2)} f\left(\frac{t}{s}\right)$$

where n_A, n_B, n_C and n_D the amounts of elementary constituents in A,B,C and D.

$s=(p_A+p_B)^2$ and $t=(p_A-p_C)^2$,

$$\frac{d\sigma}{dt}_{pp\to pp} \sim S^{-10} \quad \text{and} \quad \frac{d\sigma}{dt}_{\pi p\to \pi p} \sim S^{-8}$$

Unified description of inclusive and exclusive reactions at all momentum transfers*

R. Blankenbecler and S. J. Brodsky

$$E\,\frac{d\sigma}{d^3p}\,(A+B\to C+X)\to(p_T{}^2)^{-N}\,f\!\left(\frac{\mathfrak{M}^2}{s},\,\frac{t}{s}\right)$$

and[5,6]

$$\frac{d\sigma}{dt}\,(A+B\to C+D)\to(p_T{}^2)^{-N}\,f\!\left(\frac{t}{s}\right)$$

The entire kinematic range of high-energy inclusive reactions is illustrated on the Peyrou plot of Fig. 1. As usual we define

$$s=(p_A+p_B)^2,\quad t=(p_A-p_C)^2,$$

$$u=(p_B-p_C)^2,\quad \mathfrak{M}^2=(p_A+p_B-p_C)^2,$$

and

$$\epsilon=\mathfrak{M}^2/s\cong(1-p_{\rm c.m.}/p_{\rm max})\ ,$$

$$x_T=p_T/p_{\rm max},\quad x_L=p_L/p_{\rm max}\simeq(t-u)/s\,.$$

TABLE I. The expected dominant subprocesses for selected hadronic inclusive reactions at large transverse momentum. The second column lists the important exclusive processes which contribute to each inclusive cross section at $\epsilon\sim 0$. The basic subprocesses expected in the CIM, and the resulting form of the inclusive cross section $Ed\sigma/d^3p\sim(p_\perp{}^2)^{-N}\epsilon^P$ for $p_\perp{}^2\sim\infty$, $\epsilon\to 0$, and fixed $\theta_{\rm c.m.}$ are given in the last columns. The subprocesses that have the dominant $p_\perp$ dependence at fixed ϵ are underlined. For some particular final-state quantum numbers, the above powers of ϵ should be increased.

Inclusive process	Exclusive-limit channel	Subprocesses	$\frac{d\sigma}{d^3p/E}$ $(\theta\sim 90°)$
$M+B\to M+X$	$M+B\to M+B^*$ $(n=10)$	$\underline{M+q\to M+q}$	$(p_\perp{}^2)^{-4}\epsilon^3$
		$\bar q+B\to M+qq$	$(p_\perp{}^2)^{-6}\epsilon^1$
		$M+B\to M+B^*$	$(p_\perp{}^2)^{-8}\epsilon^{-1}$
$B+B\to B+X$	$B+B\to B+B^*$ $(n=12)$	$\underline{B+q\to B+q}$	$(p_\perp{}^2)^{-6}\epsilon^3$
		$\underline{(qq)+(qq)\to B+q}$	$(p_\perp{}^2)^{-6}\epsilon^3$
		$\underline{B+(qq)\to B+qq}$	$(p_\perp{}^2)^{-8}\epsilon^1$
		$B+B\to B+B^*$	$(p_\perp{}^2)^{-10}\epsilon^{-1}$
	$B+B\to B+B^*+M^*$ $(n=14)$	$\underline{q+q\to B+\bar q}$	$(p_\perp{}^2)^{-4}\epsilon^7$
		$q+(qq)\to B+M^*$	$(p_\perp{}^2)^{-6}\epsilon^5$
		$(qq)+B\to B+M^*+qq$	$(p_\perp{}^2)^{-10}\epsilon^1$
		$B+B\to B+B^*+M^*$	$(p_\perp{}^2)^{-12}\epsilon^{-1}$
$B+B\to M+X$	$B+B\to M+B^*+B^*$ $(n=14)$	$\underline{q+(qq)\to M+B^*}$	$(p_\perp{}^2)^{-6}\epsilon^5$
		$q+B\to q\,(\to M+q)+B^*$	$(p_\perp{}^2)^{-6}\epsilon^5$
		$q+B\to M+q+B^*$	$(p_\perp{}^2)^{-8}\epsilon^3$
		$(qq)+B\to M+B^*+qq$	$(p_\perp{}^2)^{-10}\epsilon^1$
		$B+B\to M+B^*+B^*$	$(p_\perp{}^2)^{-12}\epsilon^{-1}$
	$B+B\to M+M^*+B^*+B^*$ $(n=16)$	$\underline{M+q\to M+q}$	$(p_\perp{}^2)^{-4}\epsilon^9$
		$q+q\to\bar q\,(\to M+\bar q)+B^*$	$(p_\perp{}^2)^{-4}\epsilon^9$
		$q+q\to M+B^*+\bar q$	$(p_\perp{}^2)^{-6}\epsilon^7$
		$M+B\to M+B^*$	$(p_\perp{}^2)^{-8}\epsilon^5$
	$B+B\to M+M^*+M^*+B^*+B^*$ $(n=18)$	$\underline{q+\bar q\to M+M^*}$	$(p_\perp{}^2)^{-4}\epsilon^{11}$
		$\underline{q+M\to q\,(\to M+q)+M^*}$	$(p_\perp{}^2)^{-4}\epsilon^{11}$
$B+B\to\bar B+X$	$B+B\to\bar B+B^*+B^*+\overline{B^*}$ $(n=18)$	$\underline{q+q\to B^*+\bar q\,(\to\bar B+qq)}$	$(p_\perp{}^2)^{-4}\epsilon^{11}$
		$q+q\to B^*+\bar B+qq$	$(p_\perp{}^2)^{-8}\epsilon^7$
		$q+(qq)\to\bar B+B^*+B^*$	$(p_\perp{}^2)^{-10}\epsilon^5$

S.J. Brodsky, J.F.Gunion

August 1976
(T/E)

RECENT DEVELOPMENTS IN THE THEORY OF LARGE TRANSVERSE MOMENTUM PROCESSES*

TABLE I

Scaling Predictions for $E\, d\sigma/d^3p = C\, p_T^{-n}(1-x_T)^F$

Large p_T Process	Leading CIM Subprocess	Predicted	Observed (CP)[3]
		n//F	n//F
$pp \to \pi^+X$	$qM \to q\pi^+$	8//9	8.5//8.8
π^-	$qM \to q\pi^-$	8//9	8.9//9.7
K^+	$qM \to qK^+$	8//9	8.4//8.8
K^-	$qM \to qK^-$	8//13	8.9//11.7
	$q\bar{q} \to K^+K^-$	8//11	
$pp \to pX$	$q(qq) \to Mp$	12//5	11.7//6.8
	$qB \to qp$	12//7	
$pp \to \bar{p}X$	$q\bar{q} \to B\bar{p}$	12//11	8.8//14.2
	$qM \to qM$	8//15	
$\pi p \to \pi X$	$q\bar{q} \to M\pi$	8//5	
	$qM \to q\pi$	8//7	
	$q(qq) \to B\pi$	12//3	
	$\pi q \to \pi q$	8//3	

SLAC-PUB-9281
July 2002

Perspectives on Exclusive Processes in QCD*

Stanley J. Brodsky

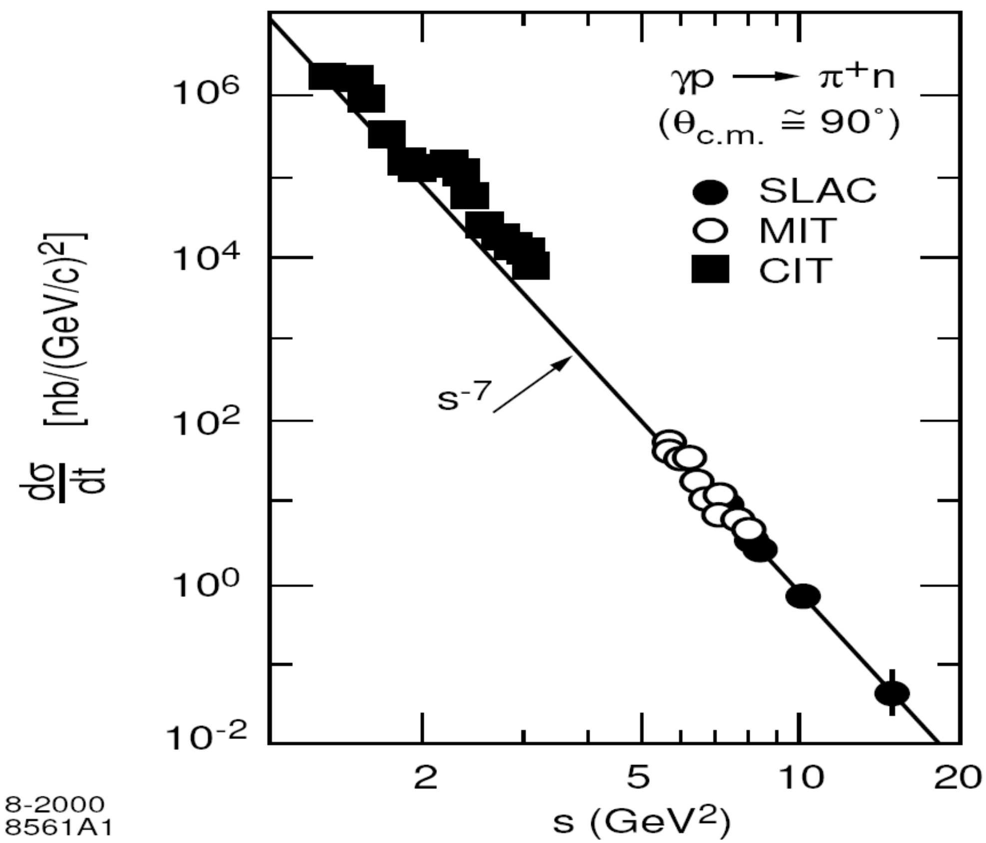

Figure 5: Comparison of photoproduction data with the dimensional counting power-law prediction. The data are summarized in Anderson *et al.*[70]

Comparison of 20 exclusive reactions at large t

TABLE I. Measured reactions presented in this paper. The reactions are written as (beam + target) → (spectrometer particle + side particle). Reactions 1, 2, 3, 17, and 18 were measured with either final-state particle in the spectrometer.

Meson-baryon reactions	
1	$\pi^+p \to p\pi^+$
2	$\pi^-p \to p\pi^-$
3	$K^+p \to pK^+$
4	$K^-p \to pK^-$
5	$\pi^+p \to p\rho^+$
6	$\pi^-p \to p\rho^-$
7	$K^+p \to pK^{*+}$
8	$K^-p \to pK^{*-}$
9	$K^-p \to \pi^-\Sigma^+$
10	$K^-p \to \pi^+\Sigma^-$
11	$K^-p \to \Lambda\pi^0$
12	$\pi^-p \to \Lambda K^0$
13	$\pi^+p \to \pi^+\Delta^+$
14	$\pi^-p \to \pi^-\Delta^+$
15	$\pi^-p \to \pi^+\Delta^-$
16	$K^+p \to K^+\Delta^+$
Baryon-baryon reactions	
17	$pp \to pp$
18	$\bar{p}p \to p\bar{p}$
19	$\bar{p}p \to \pi^+\pi^-$
20	$\bar{p}p \to K^+K^-$

TABLE V. The scaling between E755 and E838 has been measured for eight meson-baryon and 2 baryon-baryon interactions at $\theta_{\text{c.m.}} = 90°$. The nominal beam momentum was 5.9 GeV/c and 9.9 GeV/c for E838 and E755, respectively. There is also an overall systematic error of $\Delta n_{\text{syst}} = \pm 0.3$ from systematic errors of ±13% for E838 and ±9% for E755.

No.	Interaction	Cross section E838	Cross section E755	n-2 ($\frac{d\sigma}{dt} \sim 1/s^{n-2}$)
1	$\pi^+p \to p\pi^+$	132 ± 10	4.6 ± 0.3	6.7 ± 0.2
2	$\pi^-p \to p\pi^-$	73 ± 5	1.7 ± 0.2	7.5 ± 0.3
3	$K^+p \to pK^+$	219 ± 30	3.4 ± 1.4	$8.3^{+0.6}_{-1.0}$
4	$K^-p \to pK^-$	18 ± 6	0.9 ± 0.9	≥ 3.9
5	$\pi^+p \to p\rho^+$	214 ± 30	3.4 ± 0.7	8.3 ± 0.5
6	$\pi^-p \to p\rho^-$	99 ± 13	1.3 ± 0.6	8.7 ± 1.0
13	$\pi^+p \to \pi^+\Delta^+$	45 ± 10	2.0 ± 0.6	6.2 ± 0.8
15	$\pi^-p \to \pi^+\Delta^-$	24 ± 5	≤ 0.12	≥ 10.1
17	$pp \to pp$	3300 ± 40	48 ± 5	9.1 ± 0.2
18	$\bar{p}p \to p\bar{p}$	75 ± 8	≤ 2.1	≥ 7.5

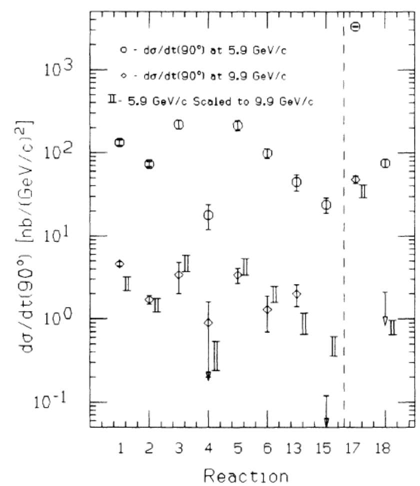

FIG. 26. The scaling between E755 and E838 has been calculated for eight meson-baryon and 2 baryon-baryon interactions at $\theta_{\text{c.m.}} = 90°$. The beam momentum for E838 was 5.9 GeV/c, corresponding to $s = 11.9$ GeV^2 for meson-baryon reactions and $s = 12.9$ GeV^2 for baryon-baryon reactions. For the 9.9 GeV/c momentum of E755, the corresponding values of s are 19.6 and 20.5 GeV^2.

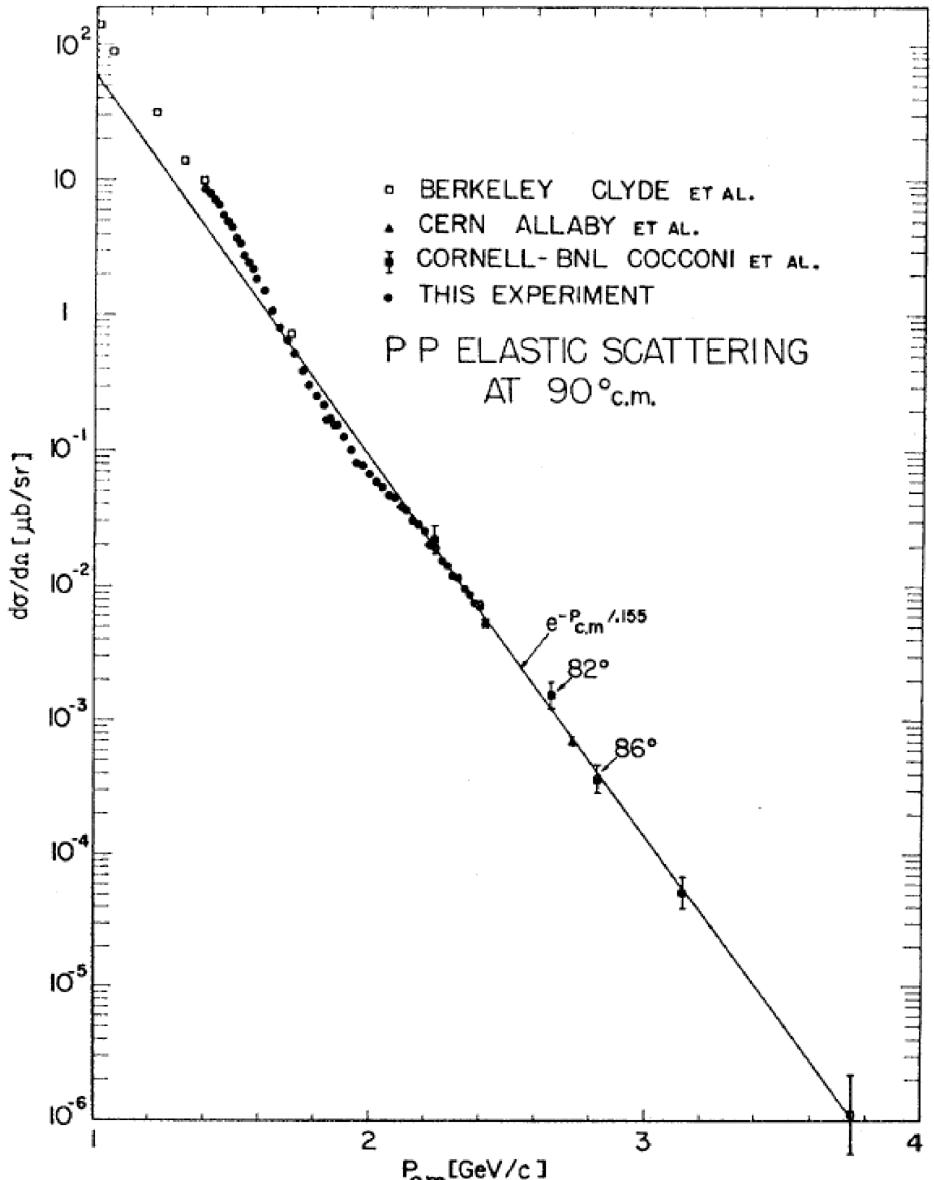

FIG. 9. Plot of $d\sigma/dt$ versus $\beta^2 P_\perp^2$ for all high-energy proton-proton elastic scattering. Other data (Refs. 13, 20, 22, 23), are also plotted. The lines drawn are straight line fits to the data.

SLAC – PUB – 4749
October 1988
(M)

ANTIPROTON ANNIHILATION IN QUANTUM CHROMODYNAMICS*

STANLEY J. BRODSKY

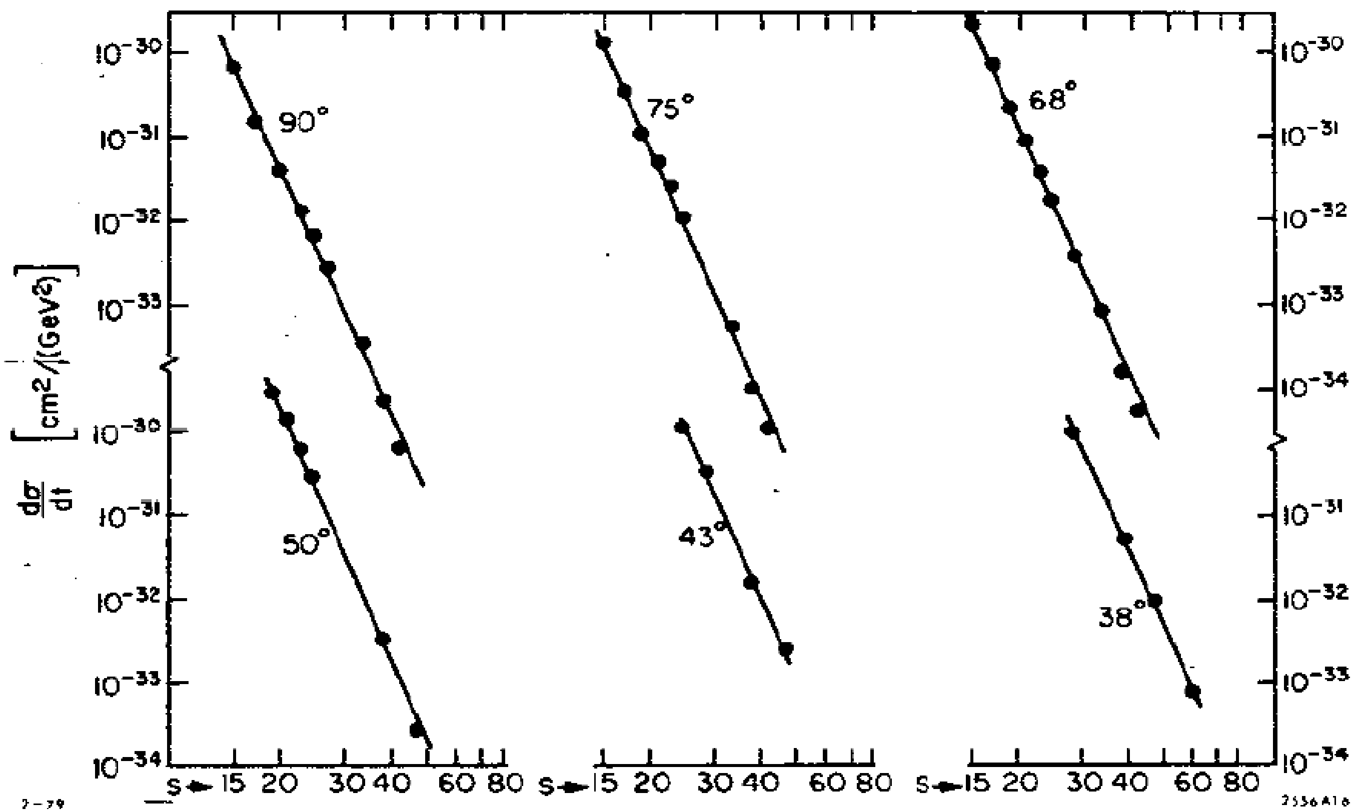

Fig. 16. Test of fixed θ_{CM} scaling for elastic pp scattering. The best fit gives the power $N = 9.7 \pm 0.5$ compared to the dimensional counting prediction $N=10$. Small deviations are not readily apparent on this log-log plot. The compilation is from Landshoff and Polkinghorne.

«ФИЗИКА ЭЛЕМЕНТАРНЫХ ЧАСТИЦ И АТОМНОГО ЯДРА»,
1984, ТОМ 15, ВЫП. 6

УДК 539.12.172

МНОГОКВАРКОВЫЕ СИСТЕМЫ В ЯДЕРНЫХ ПРОЦЕССАХ

В. В. Буров, В. К. Лукьянов, А. И. Титов

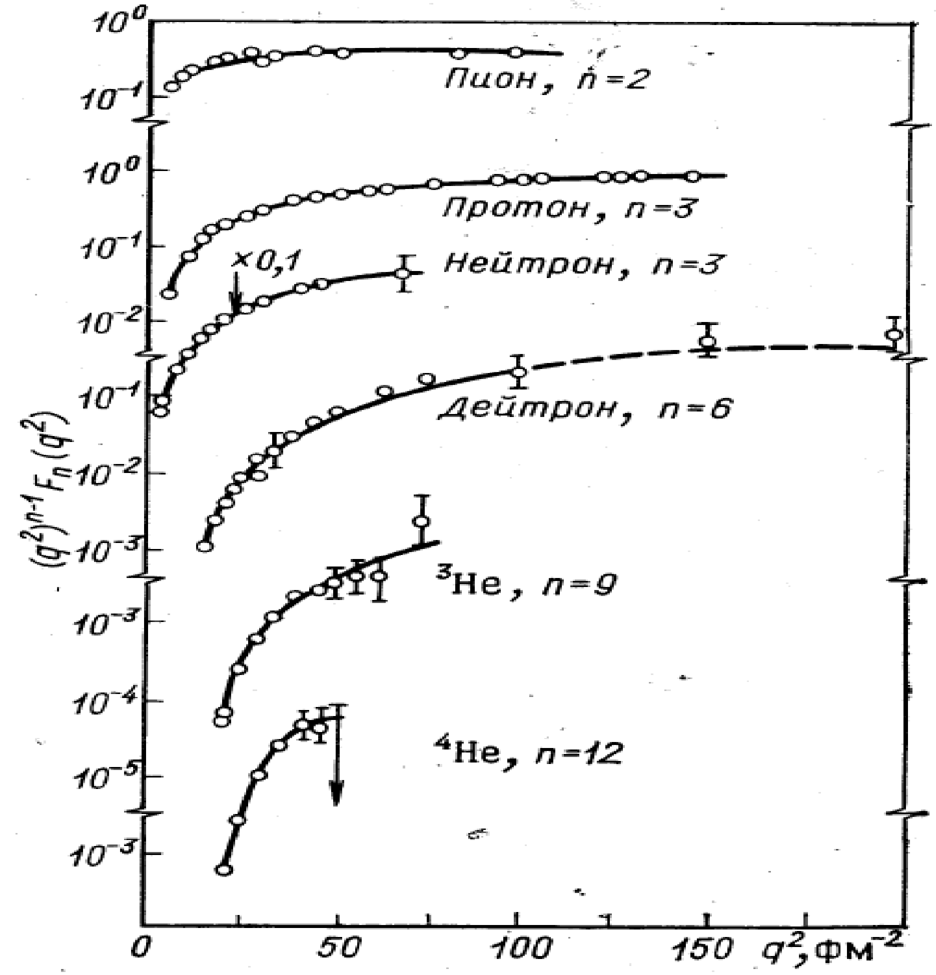

Рис. 5. Зависимость экспериментальных упругих формфакторов пиона, протона, нейтрона, дейтрона, ядер ^{3}He, ^{4}He [20, 21], умноженных на $(q^2)^{n-1}$, от q^2. Линии проведены по точкам

Which the energy range is interesting?

NN-interactions and SPIN problems (p_T~ 2 GeV/c anomaly)

pp -> pp (90^0)

C.W. Akerlof et al., Phys.Rev., vol.159, N5, 1138-1149, 1967

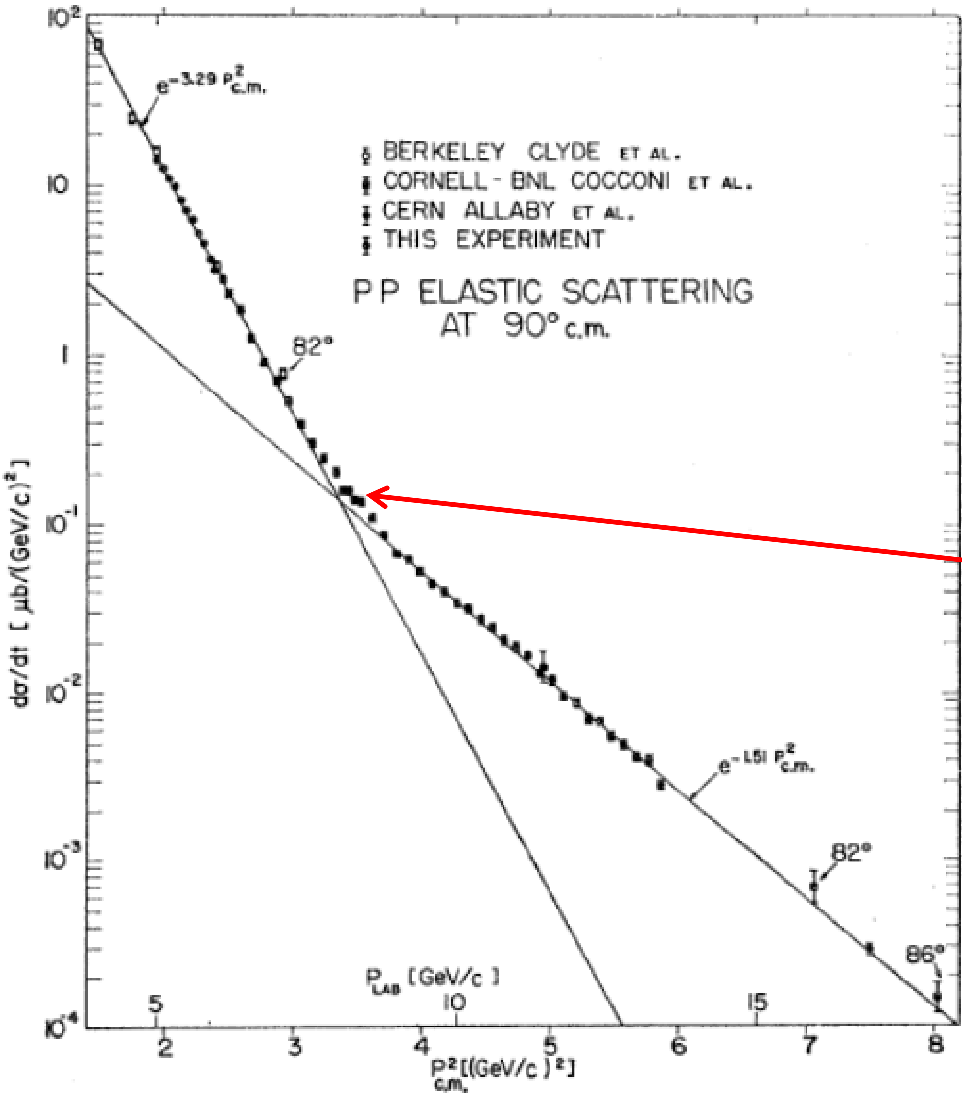

Krisch A. and Leksin G. - non pointlike structure of nucleon

p_T ~ 2 GeV/c

pp -> pp (90^0)

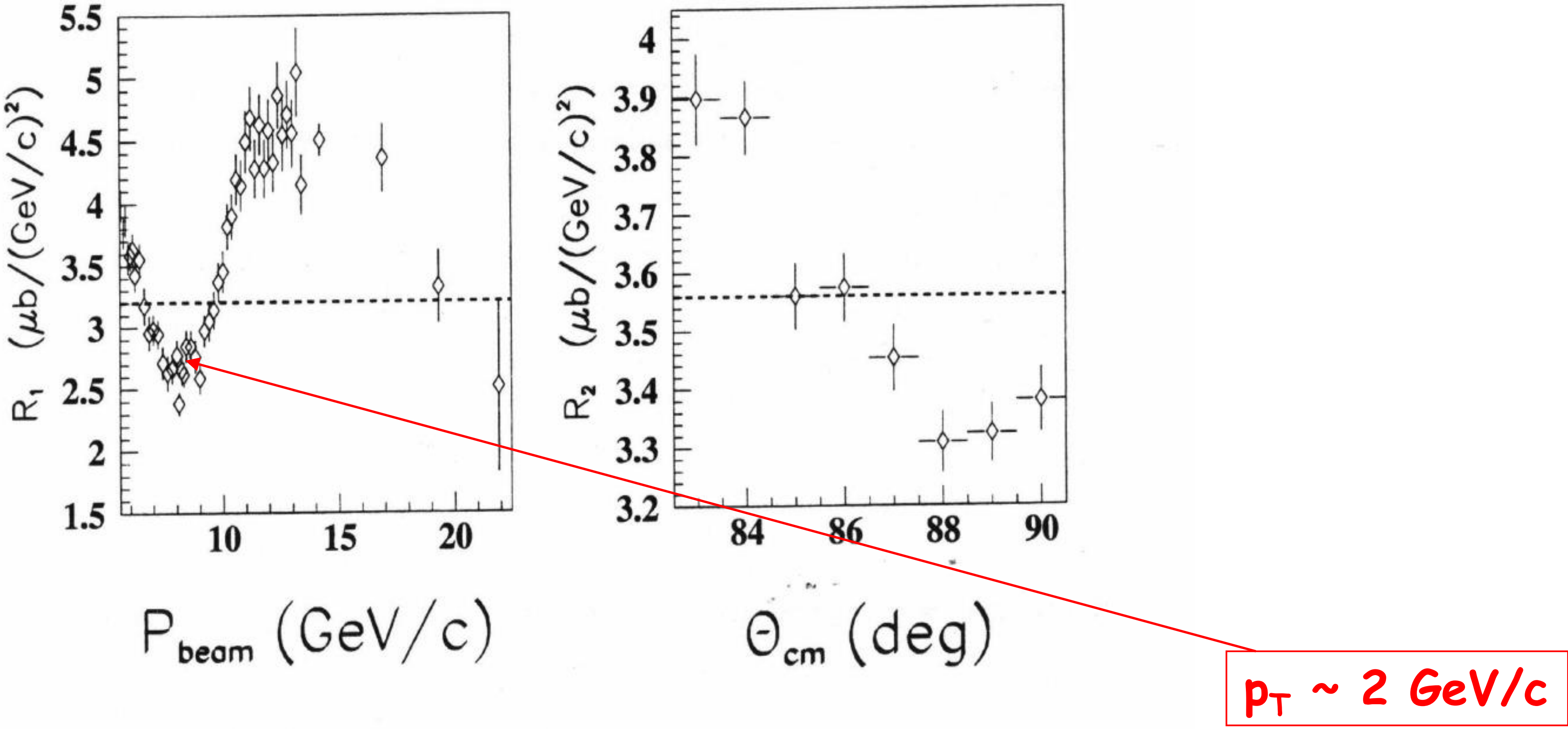

Figure 1.2: Scaled $pp \to pp$ differential cross sections. The dashed lines represent perfect scaling. Their vertical position is arbitrary. **Left** - $R_1 = \left(\left(\frac{s}{s_0}\right)^{10} \frac{d\sigma}{dt}(pp)\right)^{-1}$ ($s_0 = 13\ GeV^2$) at $\theta_{cm} = 90^0$ versus incoming momentum. Data are from Ref. [19]. **Right** - $R_2 = (1 - \cos^2\theta_{cm})^{4\gamma} \frac{d\sigma}{dt}(pp)$ ($\gamma = 1.6$) at $p_{lab} = 5.9$ GeV/c versus θ_{cm}. Data are from Ref. [17].

Color Transparency

AIP Conf.Proc. 1560 (2013) 470-474

Gerald A. Miller

Physics Department, Univ. of Washington, Seattle, Wa. 98195-1560, USA

Abstract. Color transparency is the vanishing of nuclear initial or final state interactions involving specific reactions. The reasons for believing that color transparency might be a natural consequence of QCD are reviewed. The main impetus for this talk is recent experimental progress, and this is reviewed briefly.

The basic idea is that some times a hadron is in a color-neutral point-like configuration PLC. If such undergoes a coherent reaction, in which one sums gluon emission amplitudes to calculate the scattering amplitude, the PLC does not interact with the surrounding media. A PLC is not absorbed by the nucleus. The nucleus casts no shadow. This is a kind of quantum mechanical invisibility.

Prog.Part.Nucl.Phys. 69 (2013) 1-27

Review

Color transparency: Past, present and future

D. Dutta [a,*], K. Hafidi [b], M. Strikman [c]

Color(nuclear) transparency in 90^0 c.m. quasielastic $A(p,2p)$ reactions

The incident momenta varied from 5.9 to 14.4 GeV/c, corresponding to 4.8 < Q^2 < 12.7 $(GeV/c)^2$.

$$T = \frac{\frac{d\sigma}{dt}(p + "p" \rightarrow p + p)}{Z\frac{d\sigma}{dt}(p + p \rightarrow p + p)}$$

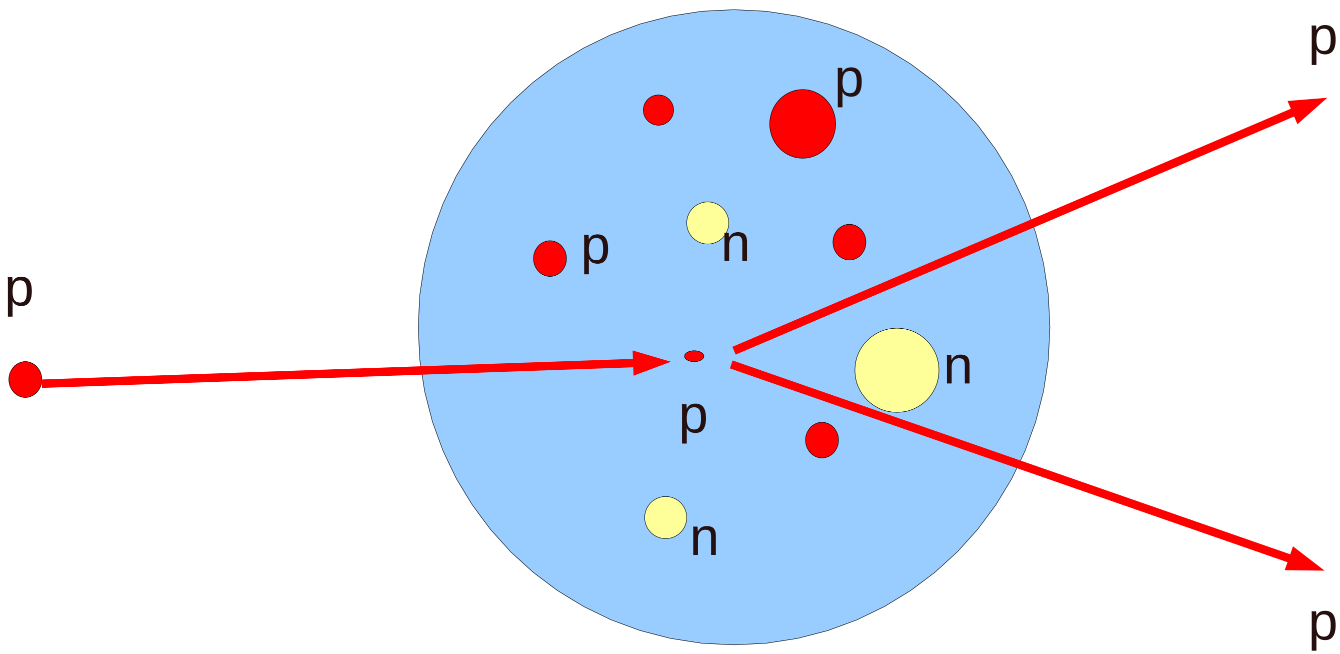

Energy Dependence of Nuclear Transparency in C(p,2p) Scattering

A. Leksanov,[5] J. Alster,[1] G. Asryan,[3,2] Y. Averichev,[8] D. Barton,[3] V. Baturin,[5,4] N. Bukhtoyarova,[3,4] A. Carroll,[3] S. Heppelmann,[5] T. Kawabata,[6] Y. Makdisi,[3] A. Malki,[1] E. Minina,[5] I. Navon,[1] H. Nicholson,[7] A. Ogawa,[5] Yu. Panebratsev,[8] E. Piasetzky,[1] A. Schetkovsky,[5,4] S. Shimanskiy,[8] A. Tang,[9] J. W. Watson,[9] H. Yoshida,[6] and D. Zhalov[5]

[1]*School of Physics and Astronomy, Sackler Faculty of Exact Sciences, Tel Aviv University, Ramat Aviv 69978, Isra*
[2]*Yerevan Physics Institute, Yerevan 375036, Armenia*
[3]*Collider-Accelerator Department, Brookhaven National Laboratory, Upton, New York, 11973*
[4]*Petersburg Nuclear Physics Institute, Gatchina, St. Petersburg 188350, Russia*
[5]*Physics Department, Pennsylvania State University, University Park, Pennsylvania 16801*
[6]*Department of Physics, Kyoto University, Sakyoku, Kyoto, 606-8502, Japan*
[7]*Department of Physics, Mount Holyoke College, South Hadley, Massachusetts 01075*
[8]*J.I.N.R., Dubna, Moscow 141980, Russia*
[9]*Department of Physics, Kent State University, Kent, Ohio 44242*
(Received 20 April 2001; published 6 November 2001)

The transparency of carbon for $(p,2p)$ quasielastic events was measured at beam momenta ranging from 5.9 to 14.5 GeV/c at 90° c.m. The four-momentum transfer squared (Q^2) ranged from 4.7 to 12.7 (GeV/c)^2. We present the observed beam momentum dependence of the ratio of the carbon to hydrogen cross sections. We also apply a model for the nuclear momentum distribution of carbon to obtain the nuclear transparency. We find a sharp rise in transparency as the beam momentum is increased to 9 GeV/c and a reduction to approximately the Glauber level at higher energies.

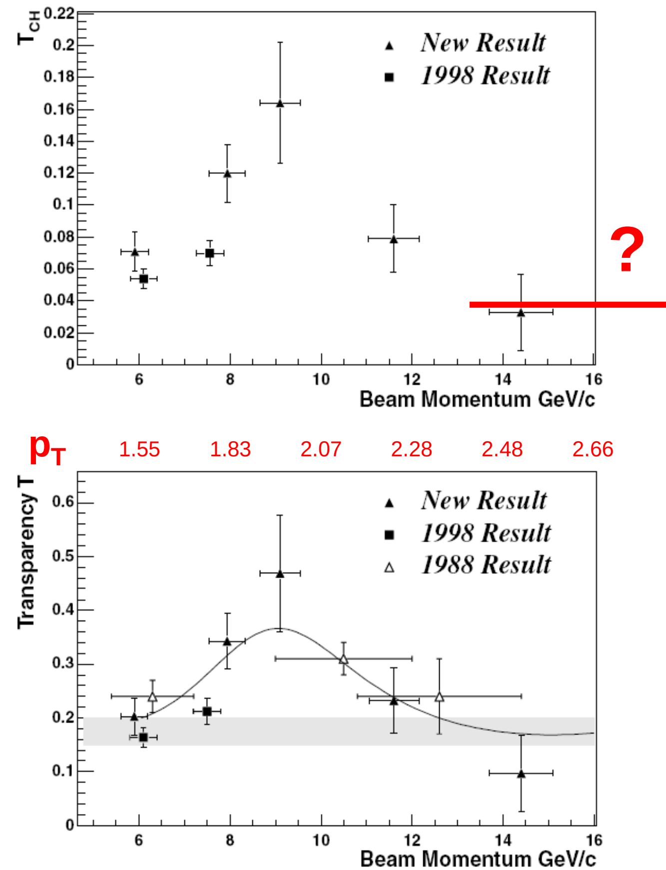

$$T_{CH} = T \int d\alpha \int d^2\vec{P}_{FT}\, n(\alpha, \vec{P}_{FT})\, \frac{(\frac{d\sigma}{dt})_{pp}(s(\alpha))}{(\frac{d\sigma}{dt})_{pp}(s_0)}$$

$$\alpha \equiv A\,\frac{(E_F - P_{Fz})}{M_A} \simeq 1 - \frac{P_{Fz}}{m_p}$$

FIG. 2. Top: The transparency ratio T_{CH} as a function of the beam momentum for both the present result and two points from the 1998 publication [3]. Bottom: The transparency T versus beam momentum. The vertical errors shown here are all statistical errors, which dominate for these measurements. The horizontal errors reflect the α bin used. The shaded band represents the Glauber calculation for carbon [9]. The solid curve shows the shape R^{-1} as defined in the text. The 1998 data cover the c.m. angular region from 86°−90°. For the new data, a similar angular region is covered as is discussed in the text. The 1988 data cover 81°−90° c.m.

$p\bar{p}$

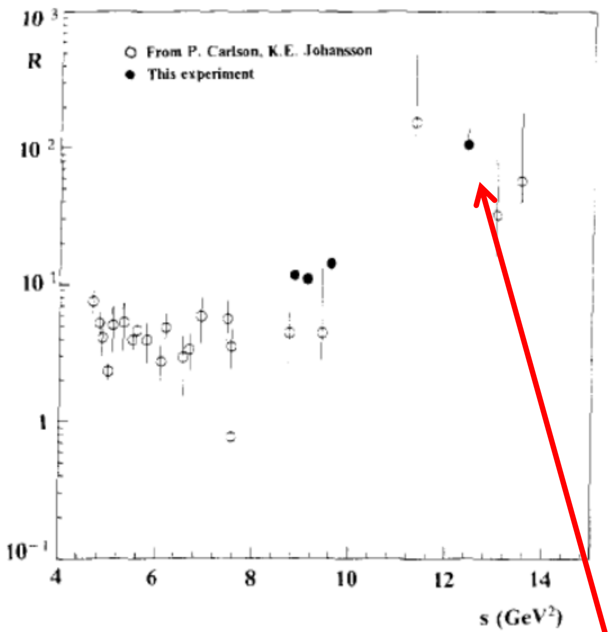

Cross-sections at 90 degrees

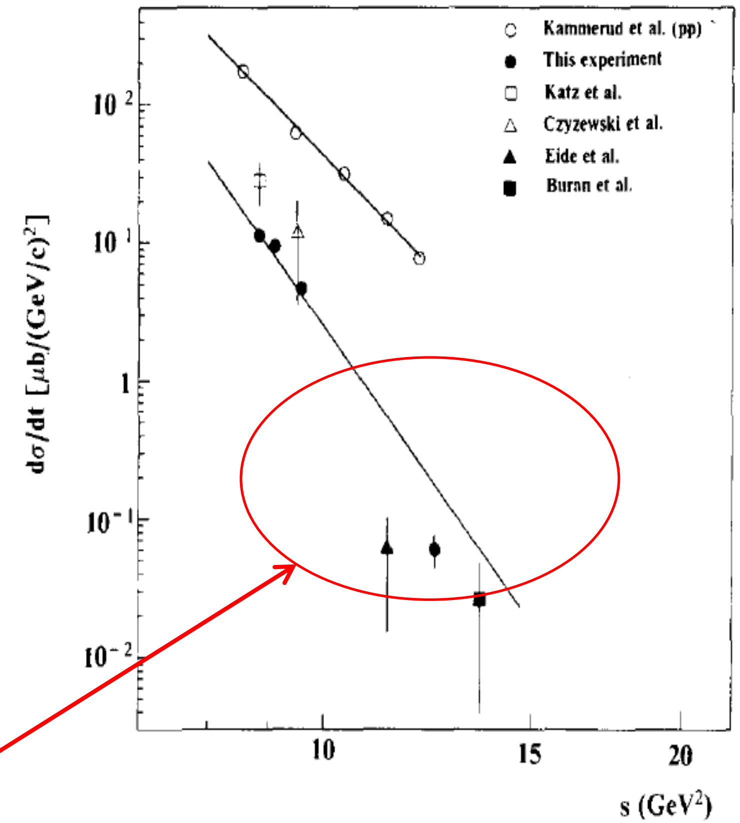

$$R = \frac{\sigma(pp \to pp)}{\sigma(\bar{p}p \to \bar{p}p)} (90^o c.m.)$$

p_T ~ 2 GeV/c region

Fig. 3. The pp̄ and pp elastic differential cross sections at 90° CM as function of the square of the CM energy, s. Open circles are pp data from ref. [6]. These data fit well to the drawn curve proportional to s^{-9}. The remaining points are pp̄ data. Shaded from this experiment. Otherwise from ref. [7] (open square), ref. [8] (open triangle) ref. [9] (shaded triangle) and ref. [10] (shaded square). The lower curve is an s^{-n} fit to four data points of this experiment, neglecting systematic errors. One obtains $n = 12.3 \pm 0.2$, but evidently the data do not seem to follow this kind of a power law.

C. Baglin et al., Phys.Lett. B, vol.225, N3, 296-300, 1989

J.W. Cronin et al., Production of hadrons at large transverse momentum at 200, 300, and 400 GeV, Phys.Rev. D, v.11, N 11, 3105-3123 (1975)

p_T ~ 2 GeV/c region

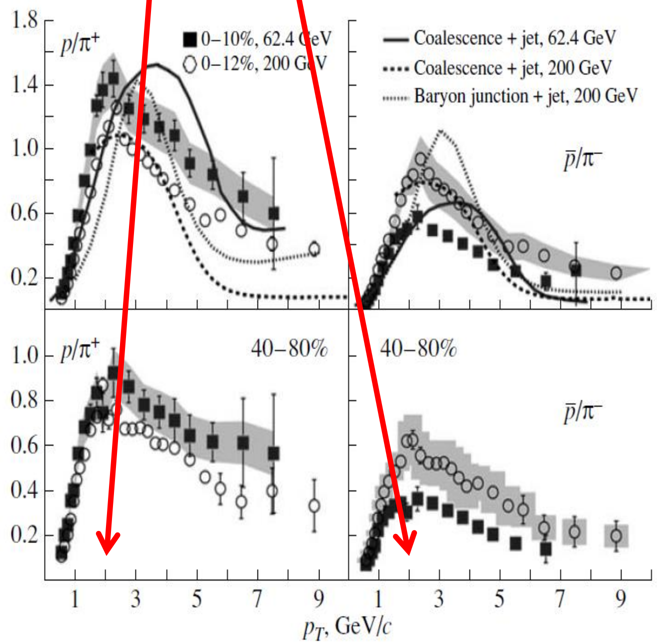

Fig. 3. [10] Ratio of the cross sections for the production of protons and charged pions as a function of the transverse momentum for various degrees of centrality and two beam energies of 62.4 and 200 GeV: (points) results of the STAR experiment and (curves) results of model calculations.

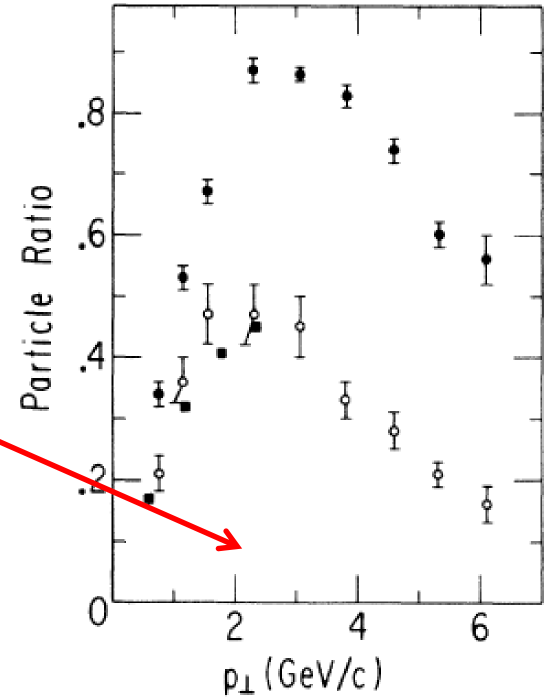

FIG. 20. Comparison of the cross-section ratio p/π^+ measured on tungsten at $\sqrt{s}=23.7$ GeV (closed circles), with that obtained by extrapolation to $A=1$ (open circles). Ratios obtained from the British-Scandinavian collaboration (Ref. 23) at $\sqrt{s}=23.4$ GeV are also plotted (closed squares).

V.S. Pantuev *Physics of Atomic Nuclei, 2009, Vol. 72, No. 12, pp. 1971–1981*

p_T~2 GeV/c anomaly at high energy (RHIC and LHC)

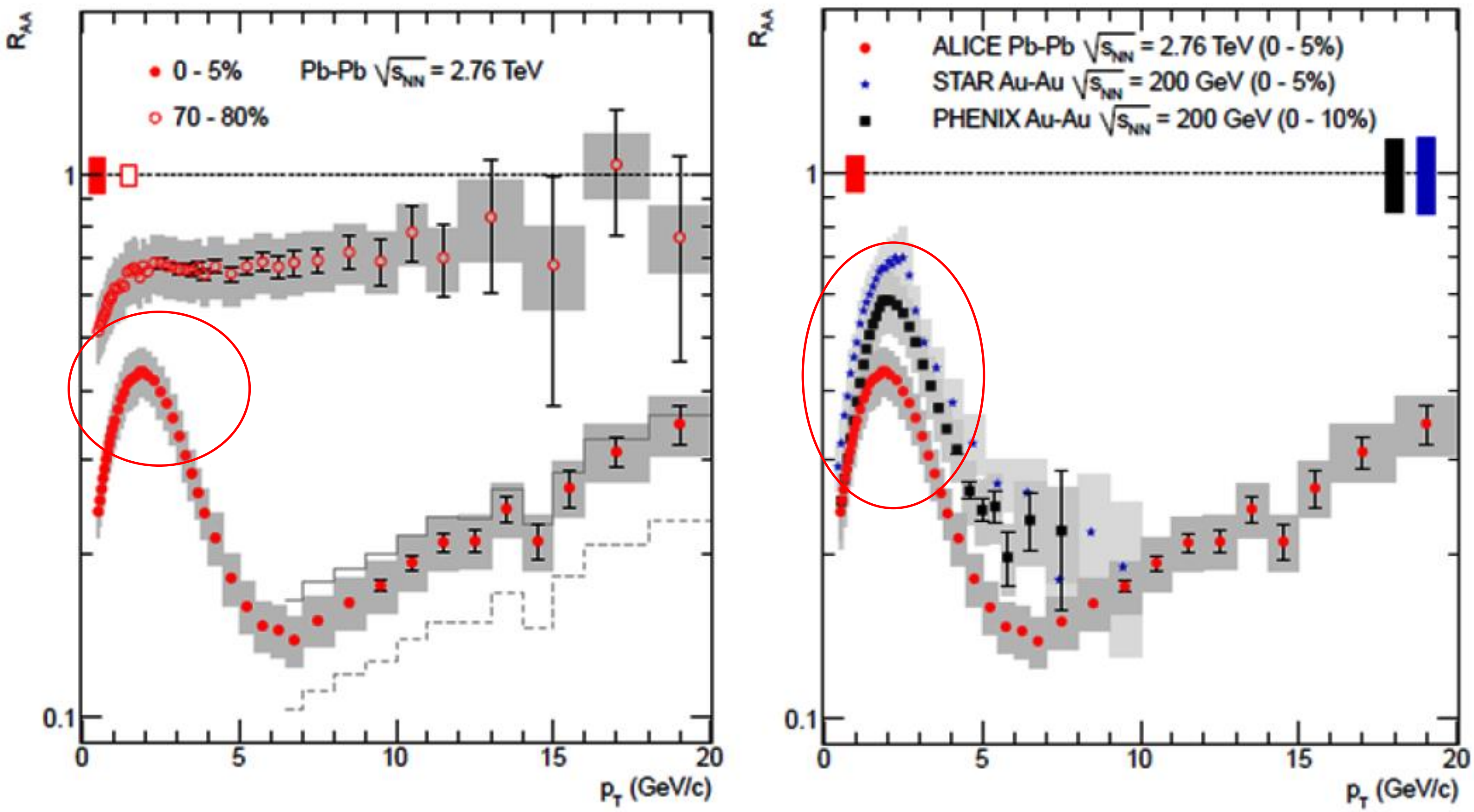

Phys. Rev. Lett. 109, 122302 (2012)

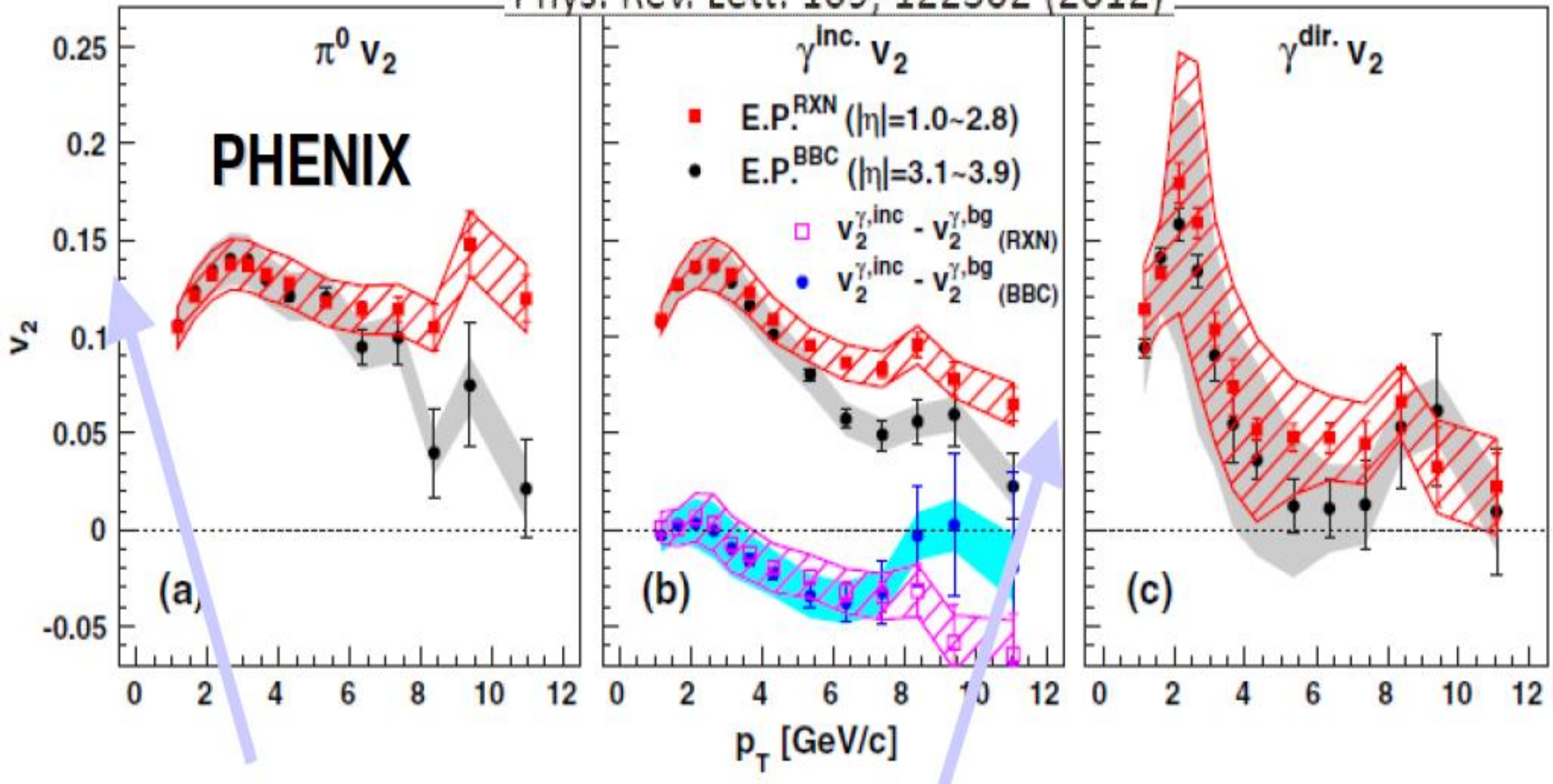

Baryon anomaly in Pb-Pb

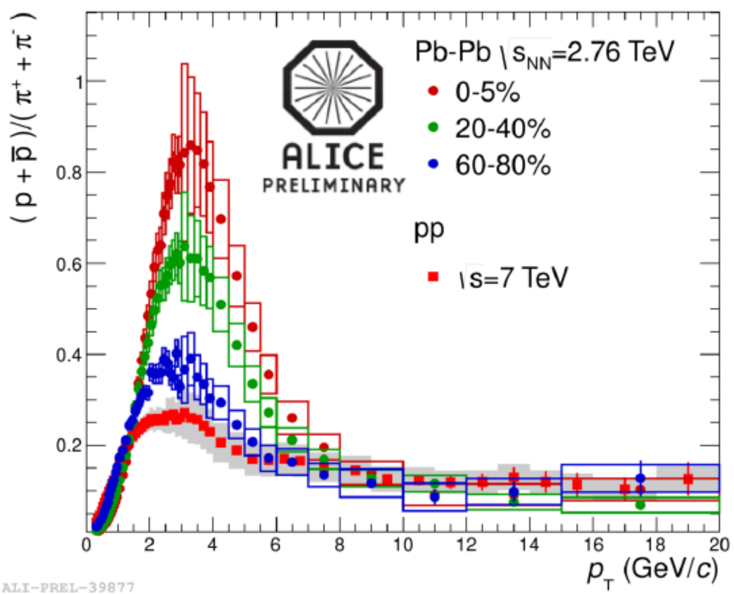

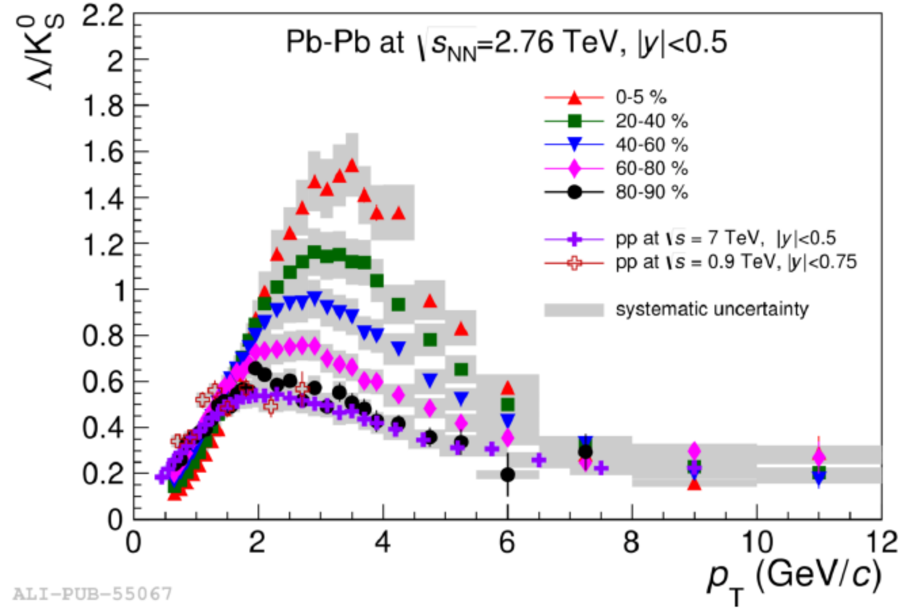

- Baryon to meson ratio increasing with centrality for $p_T < 8$ GeV/c.
  - Enhancement at moderate p_T is consistent with radial flow
  - May be explained by quark recombination from QGP (coalescence model)
- For $p_T > 8$ GeV/c no dependence on centrality and collision system
  - Consistent with fragmentation in vacuum

Nuclei and hyper-nuclei

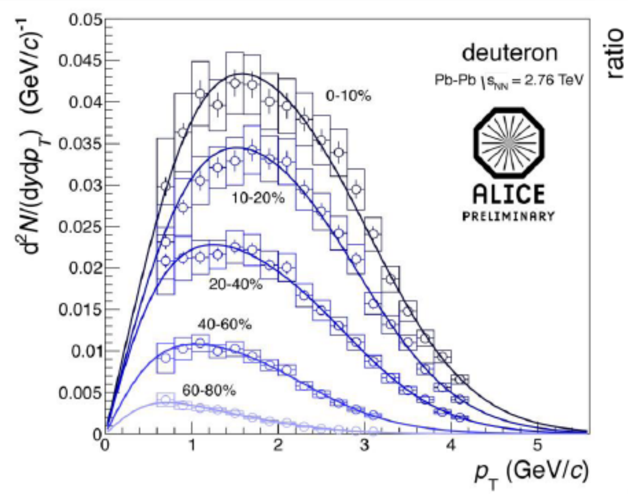

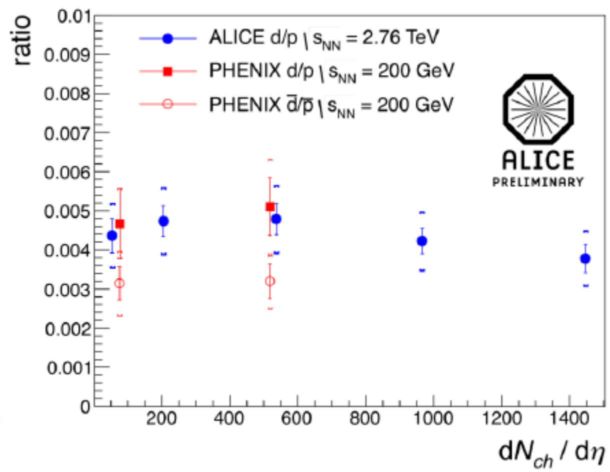

- Deuterons show hardening with increase of centrality (radial flow).
- d/p ratio does not depend on multiplcity.

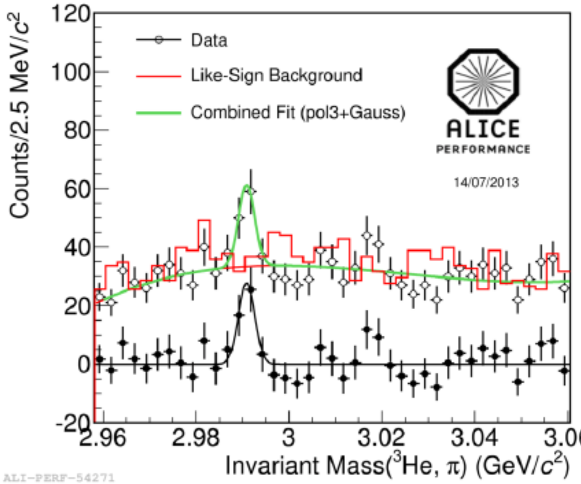

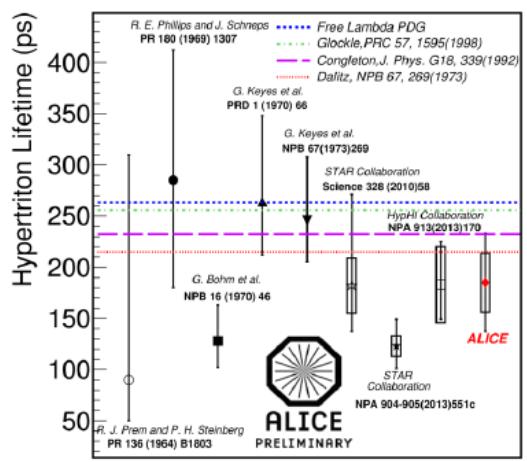

ALI-PREL-54325

- Hypertriton (p,n,Λ) yield is measured in Pb-Pb collisions.
- Production rate of $^{3}_{\Lambda}H$ is described by thermal model.
- Lifetime measured.

SPIN

Answer to Questions by Profs. Weisskopf & Bethe

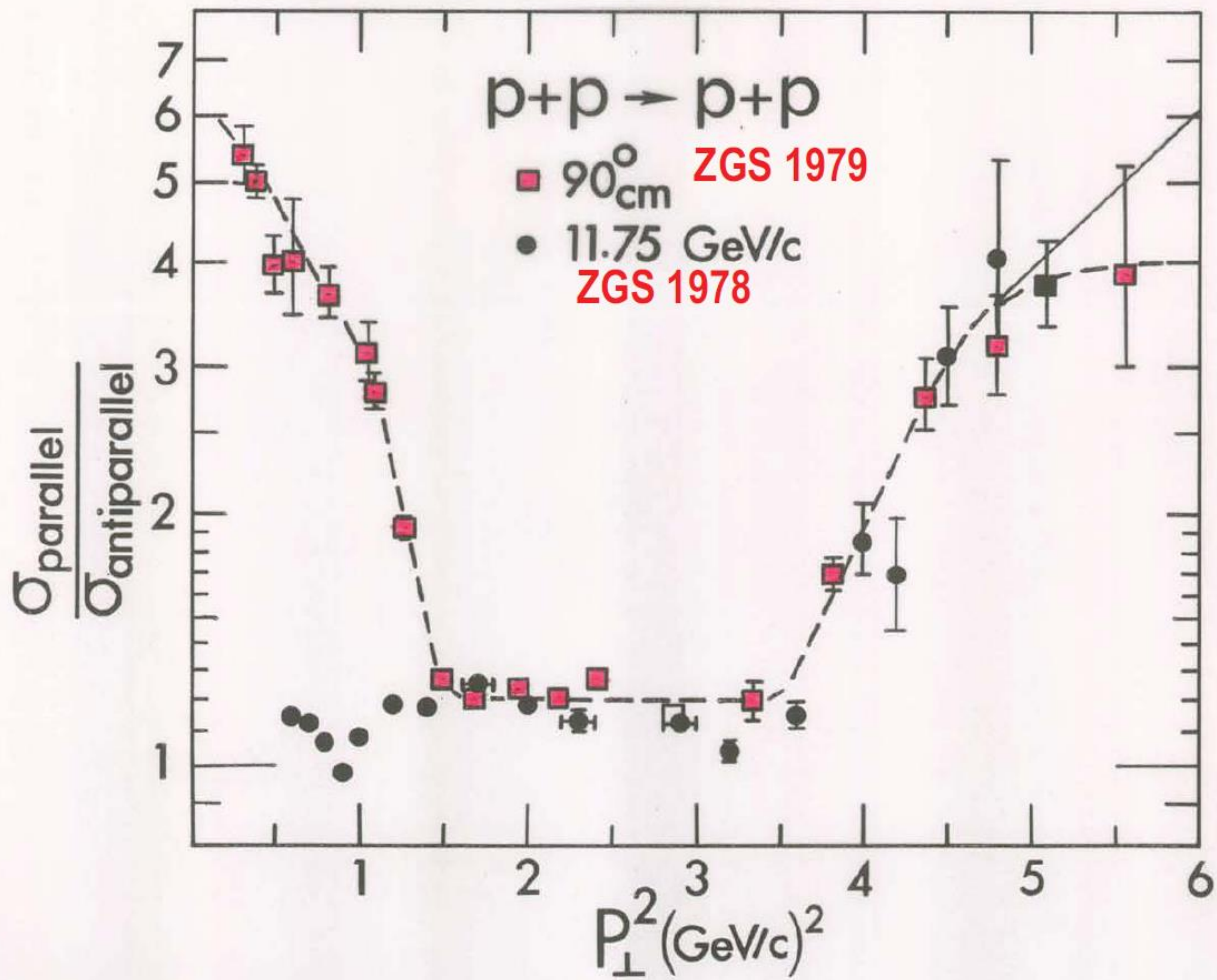

2-SPIN PROTON-PROTON ELASTIC CROSS SECTIONS

12 GeV ZGS

1977-1978

SPINS PARALLEL 4X SPINS ANTIPARALLEL

TOTALLY UNEXPECTED

Questions by Profs. Weisskopf & Bethe:

High P_T or 90^o_{cm} Identical Particles?

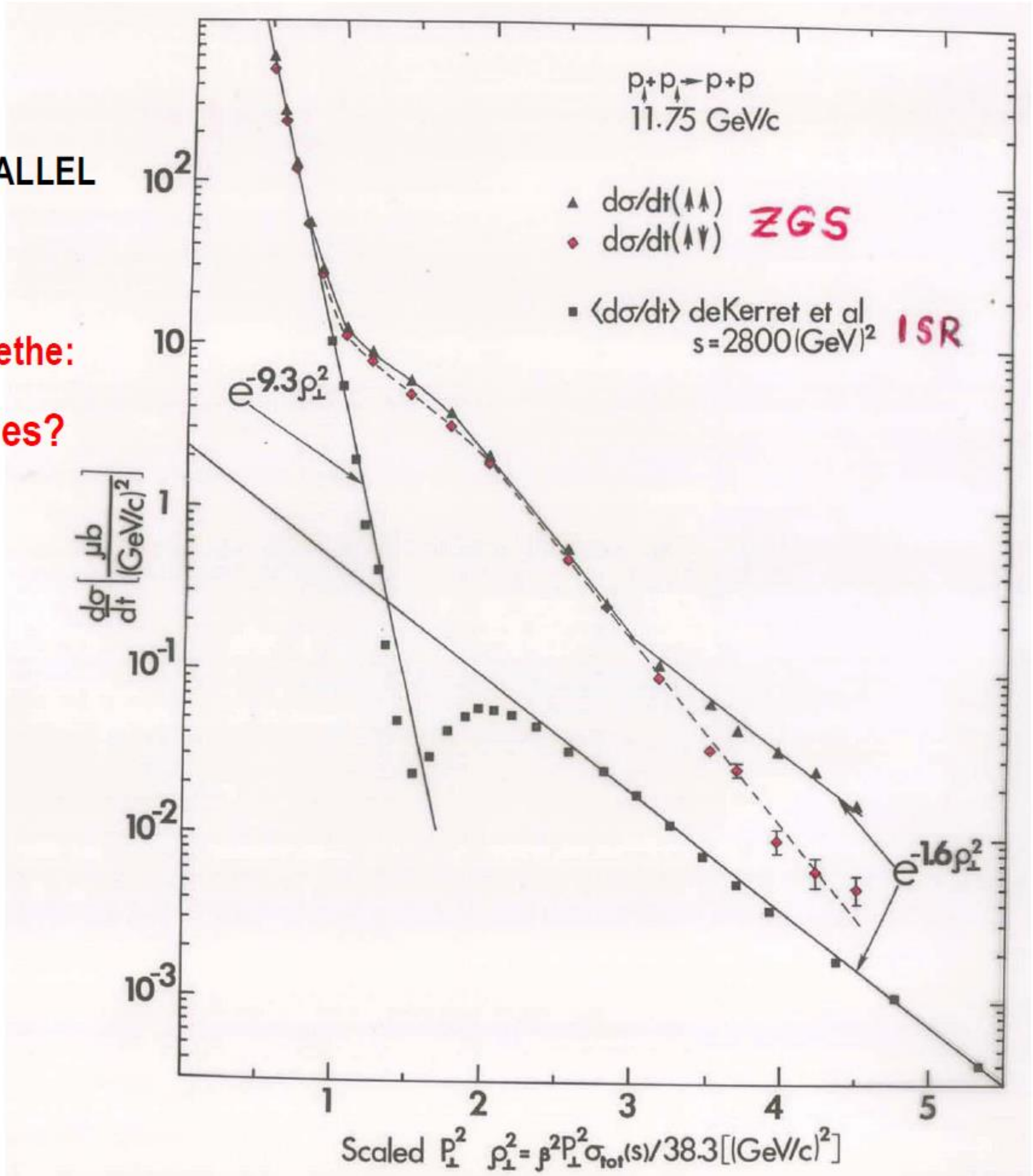

VOLUME 43, NUMBER 14 PHYSICAL REVIEW LETTERS 1 OCTOBER 1979

Spin-Spin Forces in 6-GeV/c Neutron-Proton Elastic Scattering

D. G. Crabb, P. H. Hansen, A. D. Krisch, T. Shima, and K. M. Terwilliger
Randall Laboratory of Physics, The University of Michigan, Ann Arbor, Michigan 48109

and

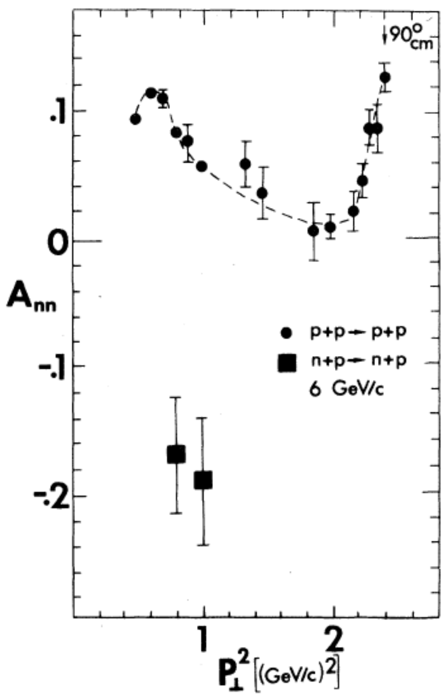

FIG. 2. The spin-spin correlation parameter, A_{nn}, for pure-initial-spin-state nucleon-nucleon elastic scattering at 6 GeV/c is plotted against the square of the transverse momentum. The proton-proton and neutron-proton data are quite different.

This large negative A_{nn} for n-p elastic scattering is quite unexpected. No theoretical models predicted this effect, although a very recent constituent-interchange model[12] predicts $A_{nn} = -44\%$. This may support the suggestion that large spin effects are related to the composite nature of the nucleon.[12,13] An earlier Regge-model prediction[14] is inconsistent with our data. It seems somewhat surprising that A_{nn} is so large at a $P_\perp{}^2$ of only 1 (GeV/c)^2.

[12]G. R. Farrar, S. Gottlieb, D. Sivers, and G. H. Thomas, Phys. Rev. D 20, 202 (1979).

AGS 1985-1990 A_n

PERTURBATIVE QCD ⇒

$A_n = 0$ at HIGH $P_\perp^2$ and HIGH ENERGY

$A_n \neq 0$ ⇒

PROBLEM with PQCD?

NO MODEL can EXPLAIN ALL

HIGH-$P_\perp^2$ SPIN EFFECTS (A_n & A_{nn})

GOAL

MEASURE A_n (and A_{nn})

up to $P_\perp^2$ = 12 (GeV/c)

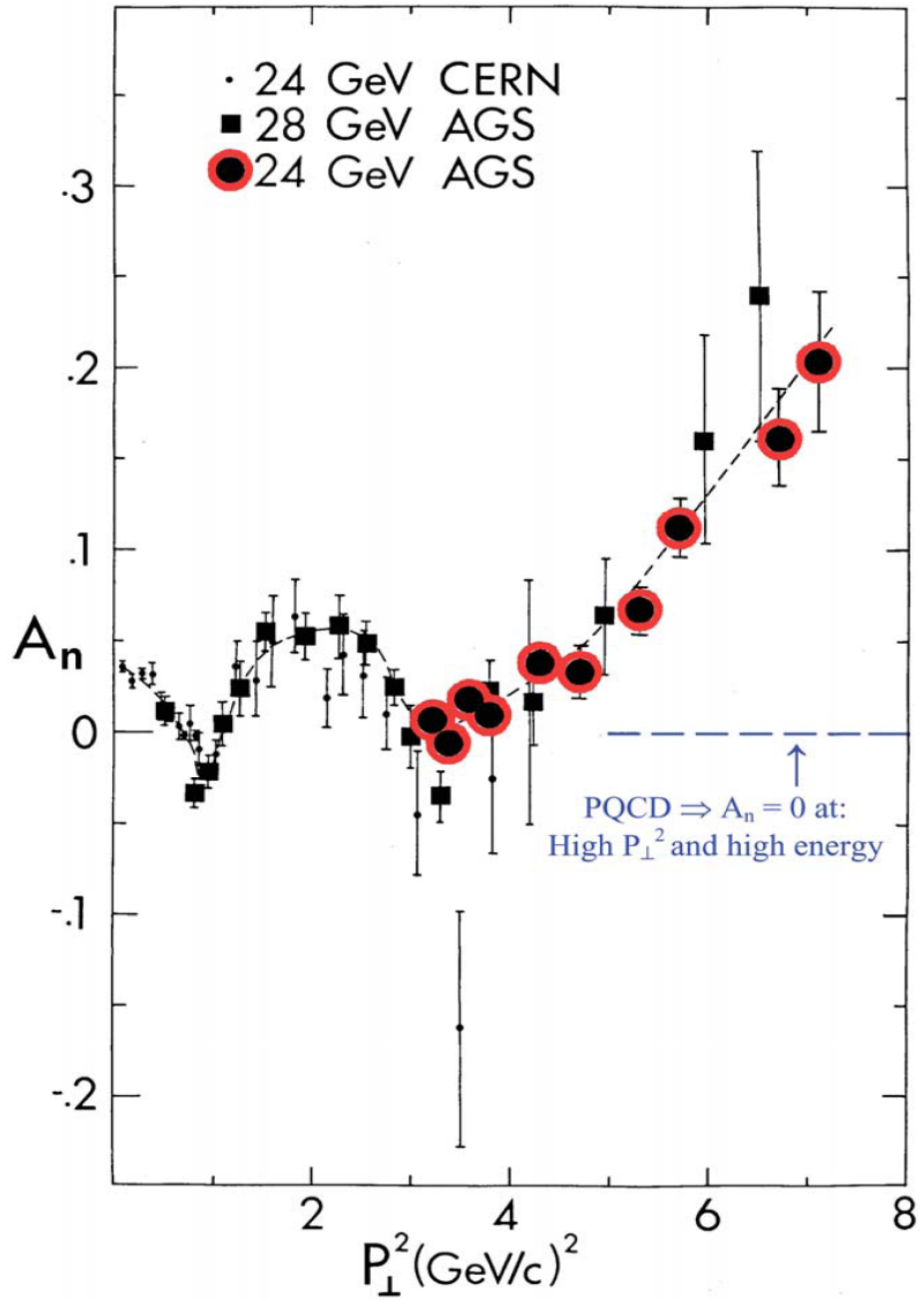

INCLUSIVE HYPERON POLARIZATION

Devlin, Pondrum, Bunce, Heller *et al.* 1976-80

Fermilab 400 GeV p+p -> Lambda ----

Plot by Heller ~1980

with KEK & ISR data

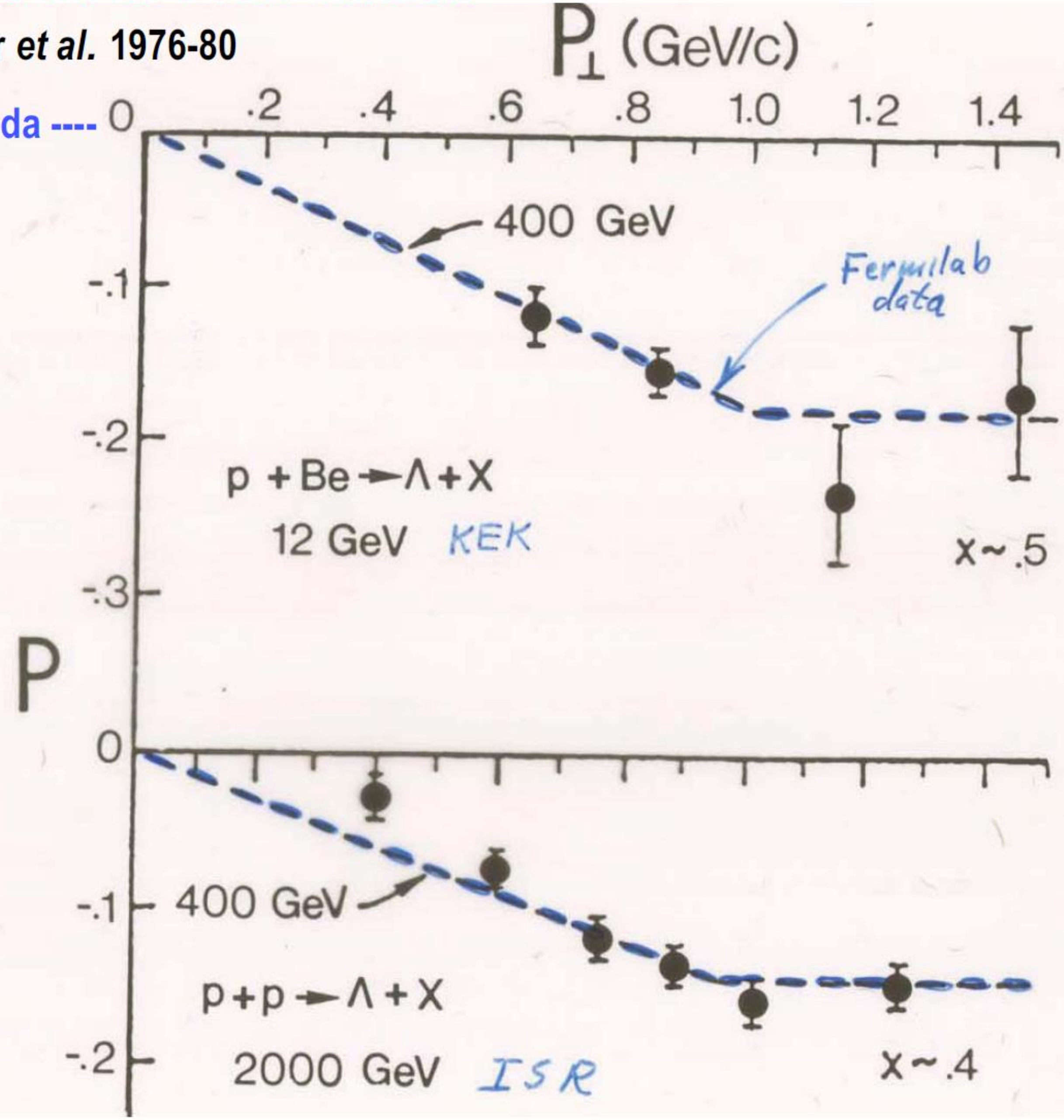

P ~ 15-20 %

QCD says P ~ 0

INCLUSIVE PION PRODUCTION

200 GeV Polarized Proton Beam

from Polarized Hyperon Decay

1990s Fermilab E-704

Yokosawa *et al*.

Phys Lett B264, 462 (1991)

$A_n \sim 40\%$

QCD said $A_n \sim 0$

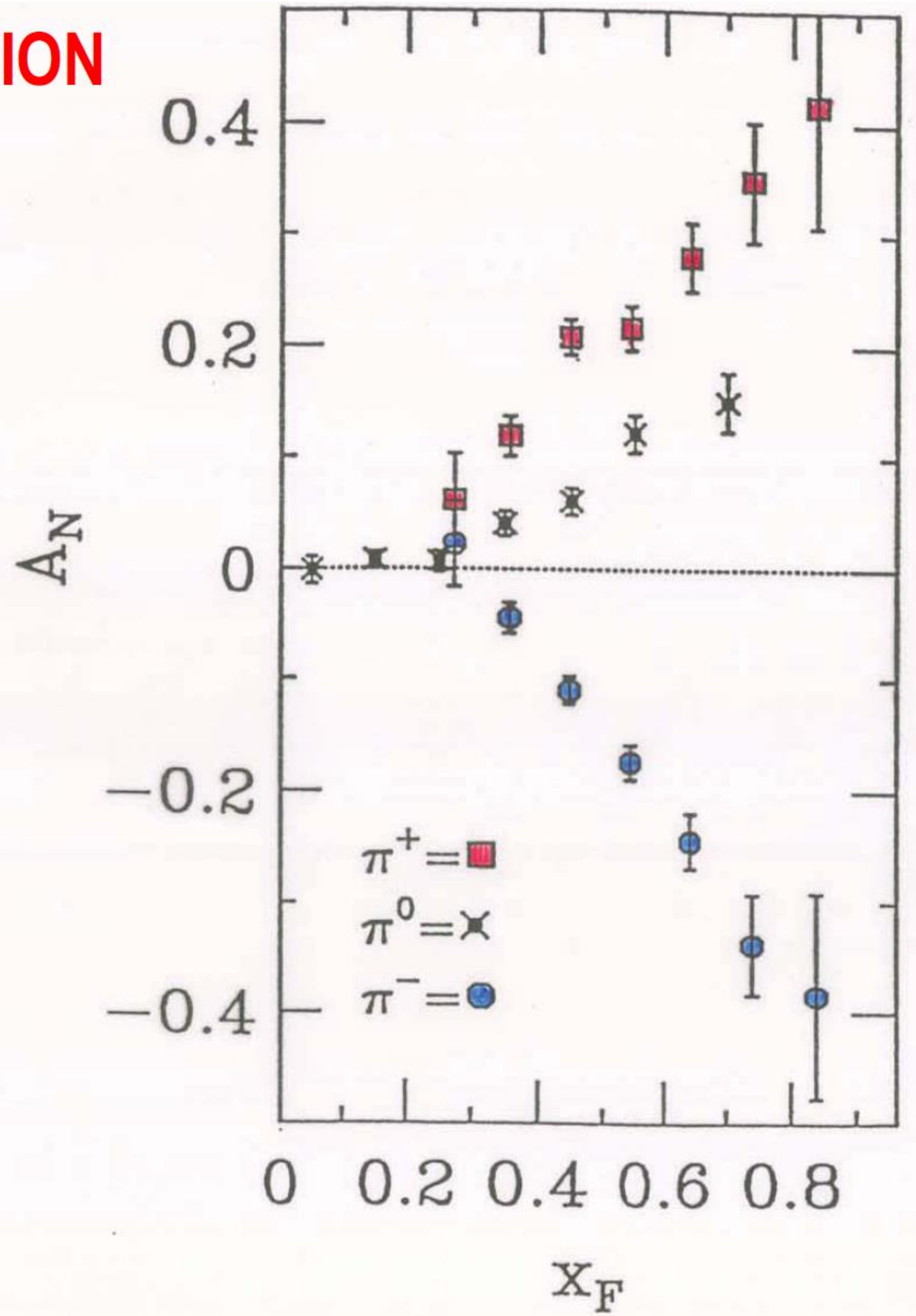

INCLUSIVE PION ASYMMETRY IN PROTON-PROTON COLLISIONS

C. Aidala SPIN 2008 Proceeding and CERN Courier June 2009

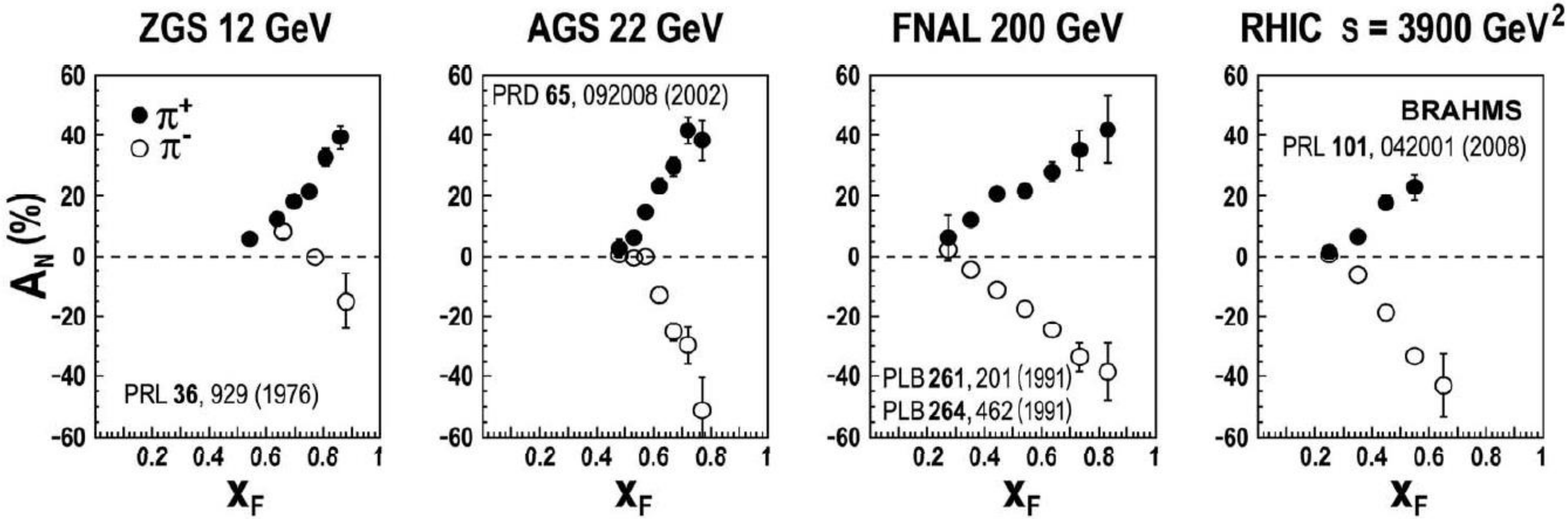

DIQUARK

Multiquark states have been discussed since the 1st page of the quark model

A SCHEMATIC MODEL OF BARYONS AND MESONS *

M. GELL-MANN
California Institute of Technology, Pasadena, California

Received 4 January 1964

If we assume that the strong interactions of baryons and mesons are correctly described in terms of the broken "eightfold way" [1-3], we are tempted to look for some fundamental explanation of the situation. A highly promised approach is the purely dynamical "bootstrap" model for all the strongly interacting particles within which one may try to derive isotopic spin and strangeness conservation and broken eightfold symmetry from self-consistency alone [4]. Of course, with only strong interactions, the orientation of the asymmetry in the unitary space cannot be specified; one hopes that in some way the selection of specific components of the F-spin by electromagnetism and the weak interactions determines the choice of isotopic spin and hypercharge directions.

Even if we consider the scattering amplitudes of strongly interacting particles on the mass shell only and treat the matrix elements of the weak, electromagnetic, and gravitational interactions by means

ber $n_t - n_{\bar{t}}$ would be zero for all known baryons and mesons. The most interesting example of such a model is one in which the triplet has spin $\frac{1}{2}$ and $z = -1$, so that the four particles d^-, s^-, u^0 and b^0 exhibit a parallel with the leptons.

A simpler and more elegant scheme can be constructed if we allow non-integral values for the charges. We can dispense entirely with the basic baryon b if we assign to the triplet t the following properties: spin $\frac{1}{2}$, $z = -\frac{1}{3}$, and baryon number $\frac{1}{3}$. We then refer to the members $u^{\frac{2}{3}}$, $d^{-\frac{1}{3}}$, and $s^{-\frac{1}{3}}$ of the triplet as "quarks" [6] q and the members of the anti-triplet as anti-quarks $\bar{q}$. Baryons can now be constructed from quarks by using the combinations (qqq), $(qqqq\bar{q})$, etc., while mesons are made out of $(q\bar{q})$, $(qq\bar{q}\bar{q})$, etc. It is assuming that the lowest baryon configuration (qqq) gives just the representations **1**, **8**, and **10** that have been observed, while the lowest meson configuration $(q\bar{q})$ similarly gives just **1** and **8**.

that it would never have been detected. A search for stable quarks of charge $-\frac{1}{3}$ or $+\frac{2}{3}$ and/or stable di-quarks of charge $-\frac{2}{3}$ or $+\frac{1}{3}$ or $+\frac{4}{3}$ at the highest energy accelerators would help to reassure us of the non-existence of real quarks.

Reviews of Modern Physics, Vol. 65, No. 4, October 1993

Diquarks

Mauro Anselmino and Enrico Predazzi

Dipartimento di Fisica Teorica, Università di Torino and Istituto Nazionale di Fisica Nucleare, Sezione di Torino, I-10125 Torino, Italy

Svante Ekelin

Department of Mathematics, Royal Institute of Technology, S-100 44 Stockholm, Sweden

Sverker Fredriksson

Department of Physics, Luleå University of Technology, S-97187 Luleå, Sweden

D. B. Lichtenberg

Department of Physics, Indiana University, Bloomington, Indiana 47405

Among the useful phenomenological ideas is the notion of a diquark. Gell-Mann (1964) first mentioned the possibility of diquarks in his original paper on quarks. Later, Ida and Kobayashi (1966) and Lichtenberg and Tassie (1967) introduced diquarks in order to describe a baryon as a composite state of two particles, a quark and diquark. Around the same time, states having some or all of the quantum numbers of diquarks were introduced in certain group-theoretical schemes by Bose (1966), Bose and Sudarshan (1967), and Miyazawa (1966, 1968).

Aside from questions of principle, lattice calculations suffer because an enormous amount of computer time is necessary to achieve very modest results. Thus, at present, calculations with lattice gauge theory are not a satisfactory substitute for calculations with phenomenological models.

Phys.Atom.Nucl. 74 (2011) 418-425

ЯДЕРНАЯ ФИЗИКА, 2011, том 74, № 3, с. 438–446

ЭЛЕМЕНТАРНЫЕ ЧАСТИЦЫ И ПОЛЯ

QUARK–DIQUARK SYSTEMATICS OF BARYONS: SPECTRAL INTEGRAL EQUATIONS FOR SYSTEMS COMPOSED BY LIGHT QUARKS

A. V. Anisovich, V. V. Anisovich*,
M. A. Matveev, V. A. Nikonov, A. V. Sarantsev, T. O. Vulfs
Petersburg Nuclear Physics Institute, Russian Academy of Sciences, Gatchina
Received May 7, 2010; in final form, August 30, 2010

PHYSICAL REVIEW D 94, 034039 (2016)

How Often Do Diquarks Form? A Very Simple Model

Richard F. Lebed*
Department of Physics, Arizona State University, Tempe, Arizona 85287-1504, USA
(Dated: June, 2016)

Starting from a textbook result, the nearest-neighbor distribution of particles in an ideal gas, we develop estimates for the probability with which quarks q in a mixed q, $\bar{q}$ gas are more strongly attracted to the nearest q, potentially forming a diquark, than to the nearest $\bar{q}$. Generic probabilities lie in the range of tens of percent, with values in the several percent range even under extreme assumptions favoring $q\bar{q}$ over qq attraction.

We have seen that the large relative size of the short-distance attraction between quarks in the color-antitriplet channel compared to the attraction between a quark and an antiquark in the color-singlet channel leads inexorably to a given quark being initially attracted to a quark rather than an antiquark a sizeable fraction of the time. We interpret this initial attraction as the seed event in the formation of a compact diquark qq rather than a color-singlet $q\bar{q}$ pair.

DIQURK DYNAMIC

Parton Distribution Function

PDF

$0 < x < 1$

probability to find a "parton" *i* of momentum $x\, p$

parton distribution function $f_i(x_i)$

p p collision = sum of parton-parton collision

$$\sigma = \int_0^a dx_1 \int_0^1 dx_2 f_i(x_1) f_i(x_2) \sigma(ij \to X)$$

but if you look closely (high Q^2), partons split further

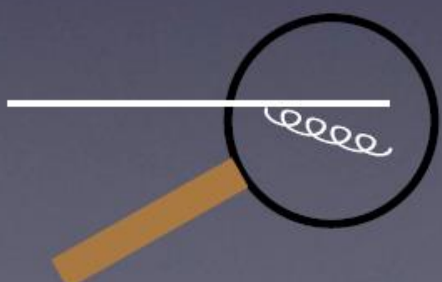

DGLAP equation

$$\frac{df_i(x)}{dQ^2} = \int_x^1 dx' f_j(x') P(j \to i + X)$$

VOLUME 5, NUMBER 1 PHYSICAL REVIEW LETTERS JULY 1, 1960

MASS ANALYSIS OF THE SECONDARY PARTICLES PRODUCED BY THE 25-GEV PROTON BEAM OF THE CERN PROTON SYNCHROTRON

V. T. Cocconi,* T. Fazzini, G. Fidecaro, M. Legros,† N. H. Lipman, and A. W. Merrison
CERN, Geneva, Switzerland
(Received June 1, 1960)

We present here some results of a mass analysis of the secondary particles produced at 15.9° to the circulating beam in an aluminum target bombarded by 25-Gev protons in the CERN proton synchrotron.

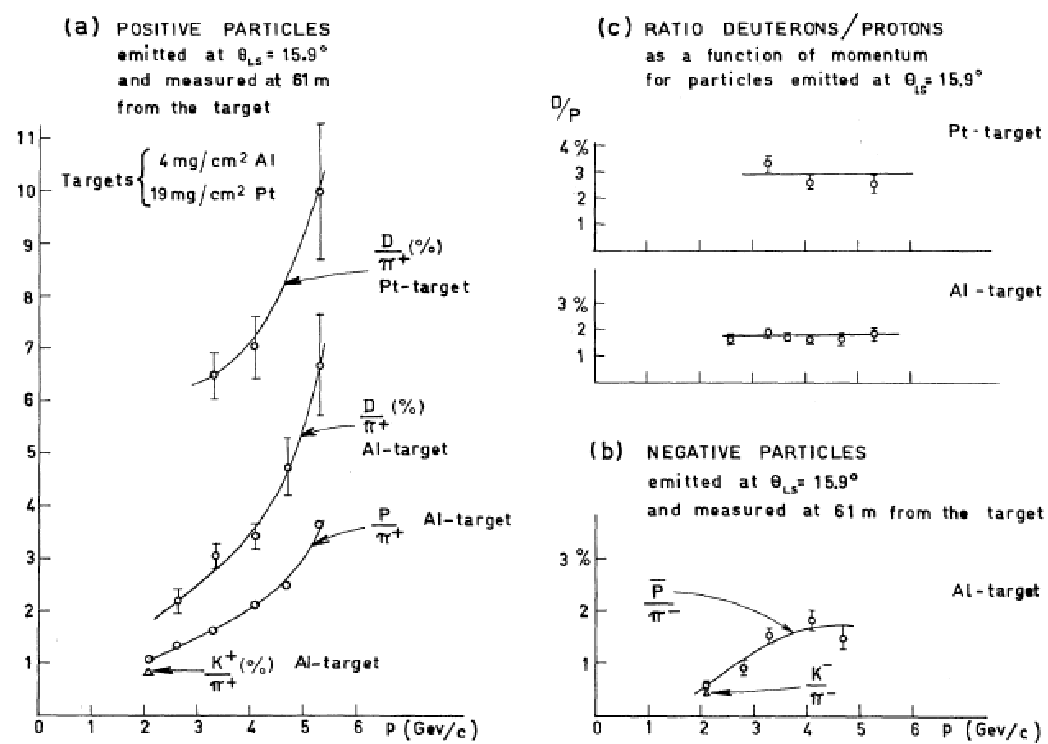

pp - > pp + X, pp -> D + X reactions with diquarks

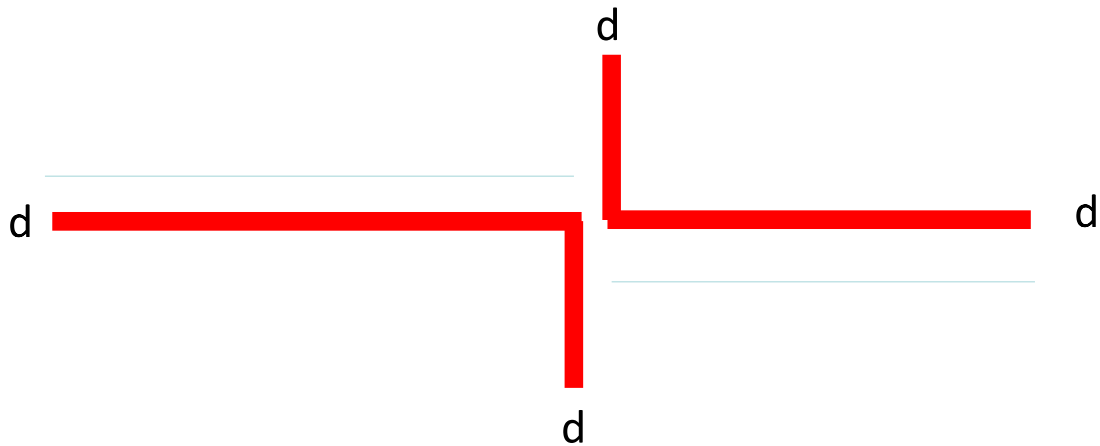

Diquark proof

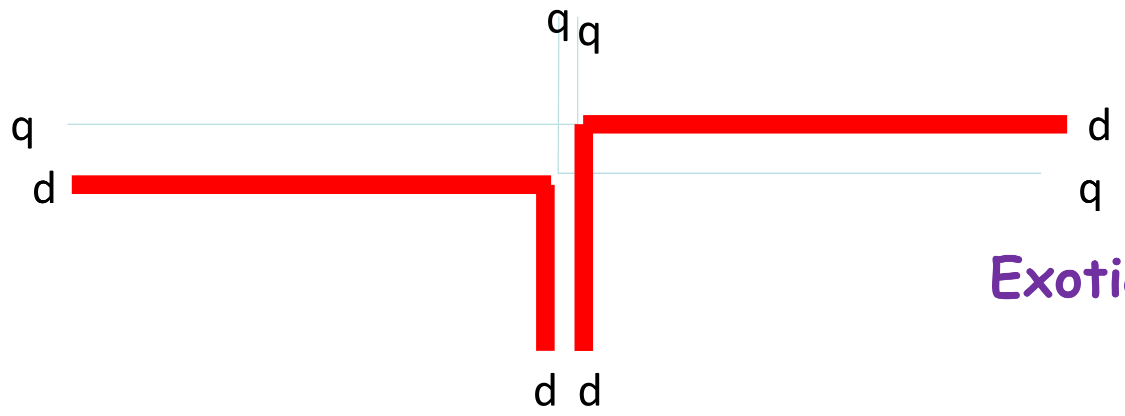

Exotic states production

Kim's mechanisms

Kim V.T. E2-87-75

Diquarks as a Source of Large-$P_\perp$ Baryons in Hard Nucleon Collisions

The production of nucleons, symmetric nucleon pairs, and Λ^o-hyperons with large $p_\perp$ in pp-collisions is discussed in the framework of a dominatiing scalar (ud)-diquark nucleon model. The necessity of making allowance for higher twists-diguarks for explaining strong scaling breaking in p/π^+ ratio is shown. The approximate equation $\Lambda/p \simeq k^+/\pi^+$ is predicted in this model.

The investigation has been performed at the Laboratory of Theoretical Physics, JINR.

Preprint of the Joint Institute for Nuclear Research. Dubna 1987

Diquarks

pp -> p+X, pp -> pp+X

V.T. Kim (1987)

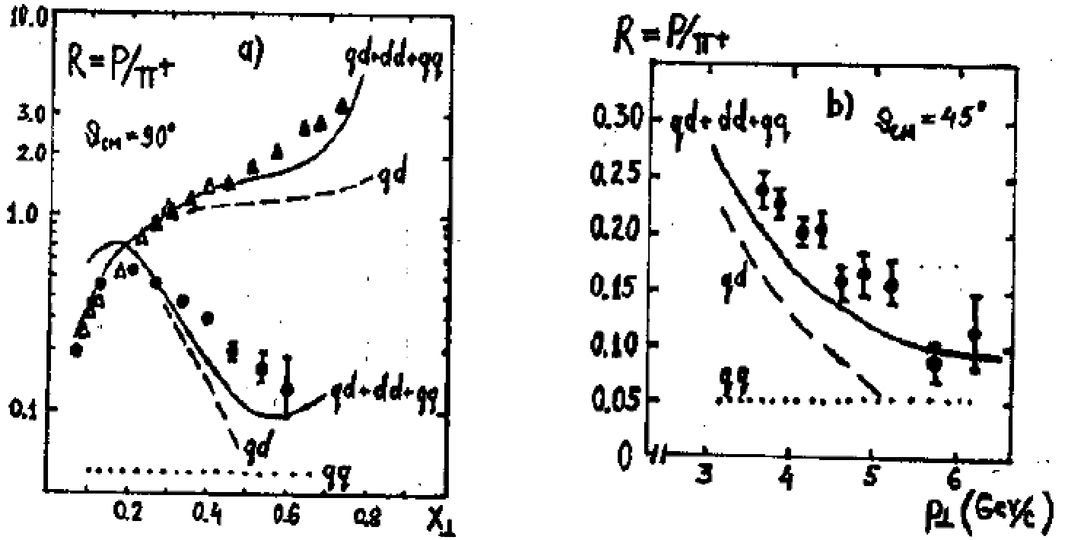

Fig. 1. $R = P/\pi^+$ -ratio in pp-collisions. a) $\vartheta_{cM} = 90°$: ● – FNAL data /16/ at $\sqrt{s} = 23.4$ GeV (E_L = 300 GeV); Δ , ▲ – IHEP (Serpukhov) data/19,20/ at $\sqrt{s}$ = 11.5 GeV (E_L = 70 GeV). b) $\vartheta_{cM} = 45°$: ● – ISR CERN data /18/ at $\sqrt{s}$ = 62 GeV ($E_L \simeq$ 1900 GeV).

The result of calcuations of $pp \to ppX$ processes/29/ (symmetric -proton-pair production) according to the formula in work/30/ for the double inclusive cross section, which in general must be applied carefully/31/ , is shown in Fig.2. The main contribution to the cross section of production of proton pairs with transverse momenta opposite and equal in values is given by diquark-diquark scattering.

arXiv:1007.4705v5 [hep-ph] 25 Sep 2010
&Phys.Rev. C83 (2011) 054606
Carlos Granados and Misak Sargsian

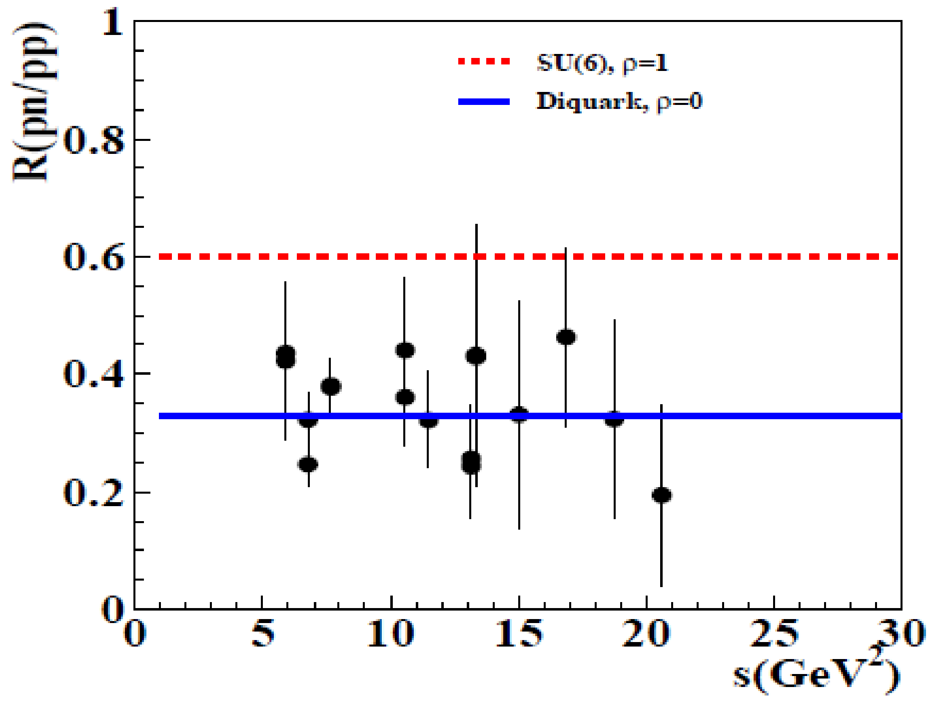

FIG. 2: (Color online) Ratio of the $pn \to pn$ to $pp \to pp$ elastic differential cross sections as a function of s at $\theta^N_{c.m.} = 90^0$.

How can we prove the existence of diquarks and determine their properties?

NN Elastic scattering with polarized deuteron beams :

$$p\uparrow + p\uparrow \to p + p$$

for calibration

$$p\uparrow + n\uparrow \to p + n$$

$$n\uparrow + n\uparrow \to n + n$$

New data!

By the way we will have the counting rules verification!

pd, nd and dd – too!

Exclusive NN study at $x_T \sim 1$

$$N\uparrow + N\uparrow \to BB + MM$$

$B\ (p, n, \Lambda, \Delta\ldots),\ M\ (\pi, K, \ldots)$

Mechanisms of hyperons polarization

$$N\uparrow N\uparrow \to NN$$

The counting rules and isotopic symmetry studies, $p_T \sim 2$ GeV/c anomaly

$$N\uparrow N\uparrow \to BB + \pi\pi(KK)$$

$$N\uparrow N\uparrow \to \Delta\Delta$$

Detail vertexes studies and spin structure of the interaction vertex:

$q + (q) - (quark - quark)$

$q + (qq) - (quark - diquark)$

$(qq) + (qq) - (diquark - diquark)$

Way to resolve these problems MPI and Exclusive reaction

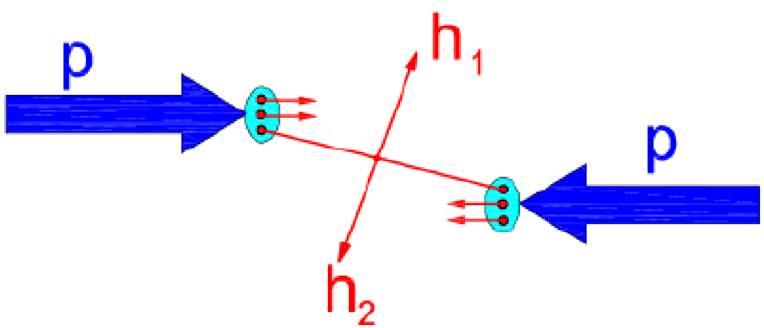

а

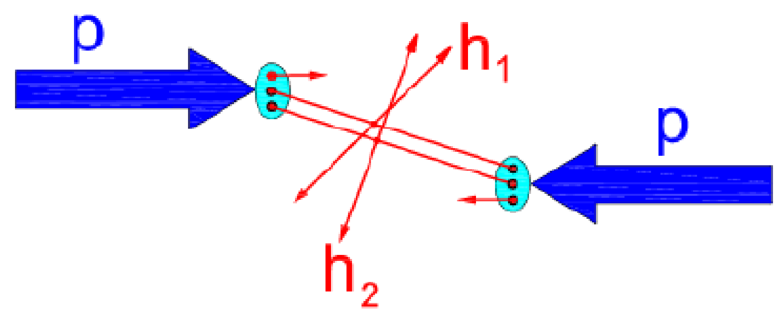

б

High p_T exclusive reactions -> MPI

$$p\uparrow + p\uparrow \to B + B + M\overline{M}$$

$$p\uparrow + p\uparrow \to p + p + \pi^0\pi^0(\pi^+\pi^-)$$

$$R = \frac{N(\pi^+\pi^-)}{N(\pi^0\pi^0)} = \frac{2}{7}$$ Without diquark

$$R = \frac{N(\pi^+\pi^-)}{N(\pi^0\pi^0)} \to 0$$ diquark

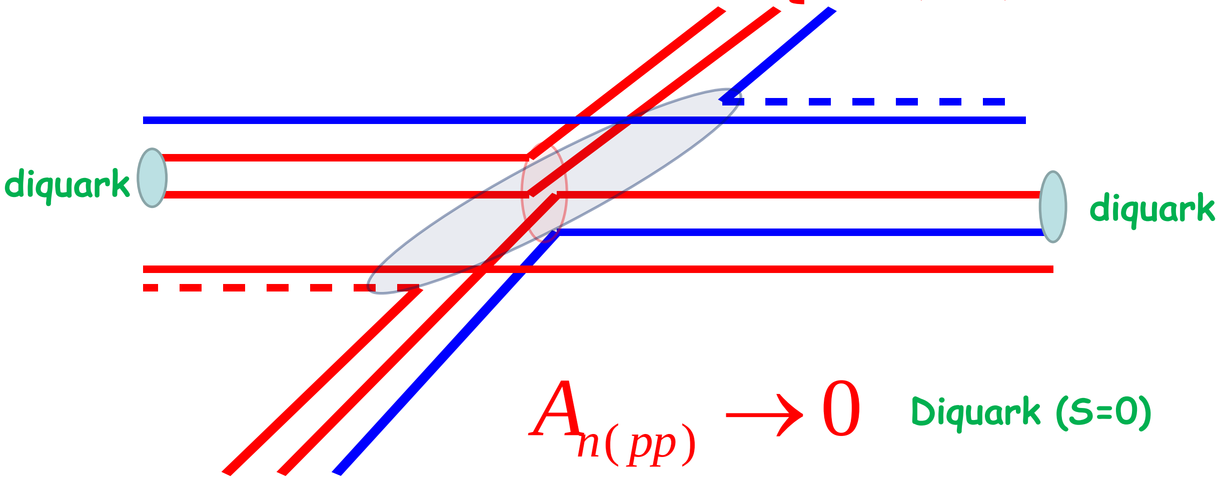

$$A_{n(pp)} \to 0$$ Diquark (S=0)

Exotic states and flavor universality

Status of the pentaquark problem

- 1^{st} relatively certain theoretical suggestion
  of mass ~1530 MeV and width < 15 MeV :

  Diakonov, Petrov, Polyakov, Z.Phys., A**359** (1997) 305.

- Experiment : about ten papers with positive evidences;
  about ten papers with negative results
  (some of them with higher statistics).

- Common opinion and PDG position
  (since edition of 2008) :

  Pentaquark is dead !

  (Note, at the same time, great enthusiasm
  in searches for tetraquarks !)

Hadrons from diquarks?

STATIC

Still an open question!

Role of diquarks in building hadrons?

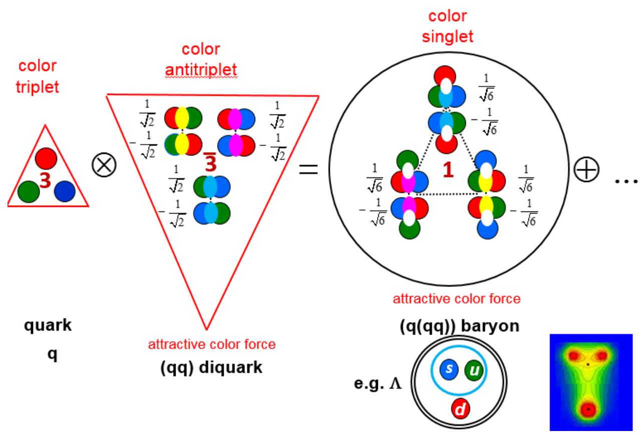

vs.

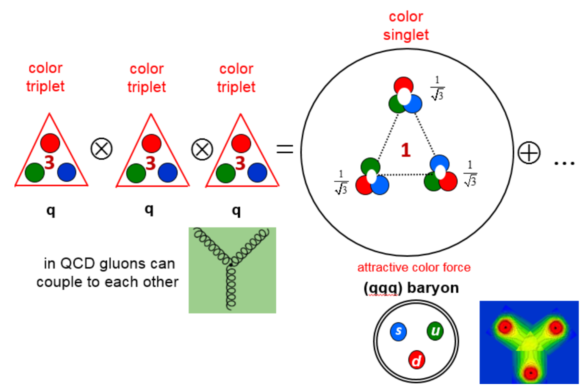

Light and heavy baryon spectroscopy is sensitive to this question

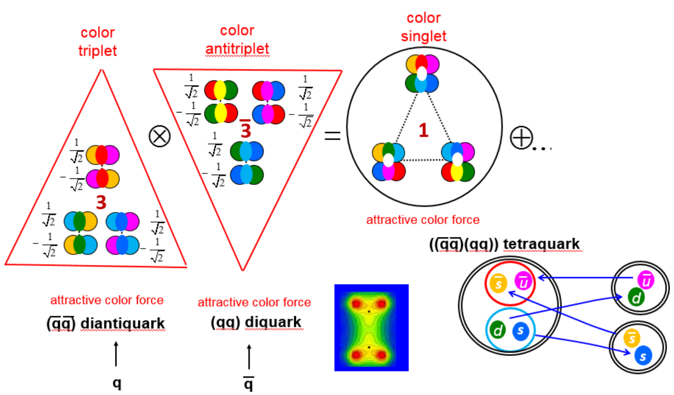

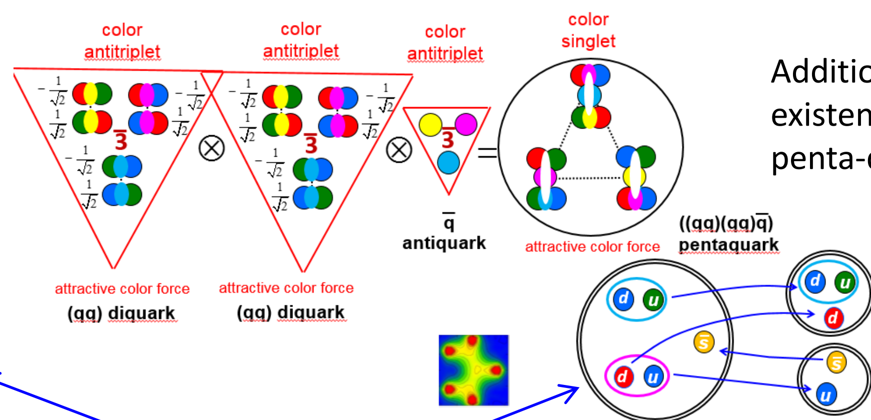

Additional motivation for existence of tetra- and penta-quarks.

Does effective mechanism to suppress rapid fall-apart exist?

pp - reactions with diquarks and тетракварки

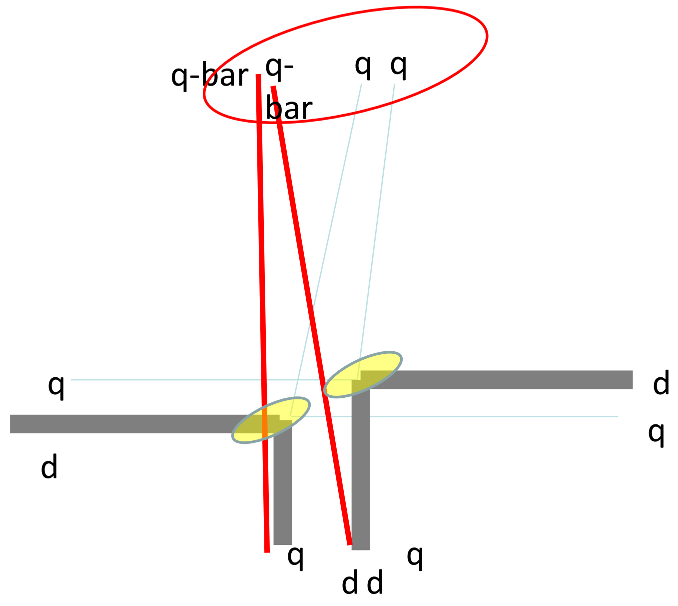

Kim's mechanisms

pp - reactions with pentaquarks production and ...

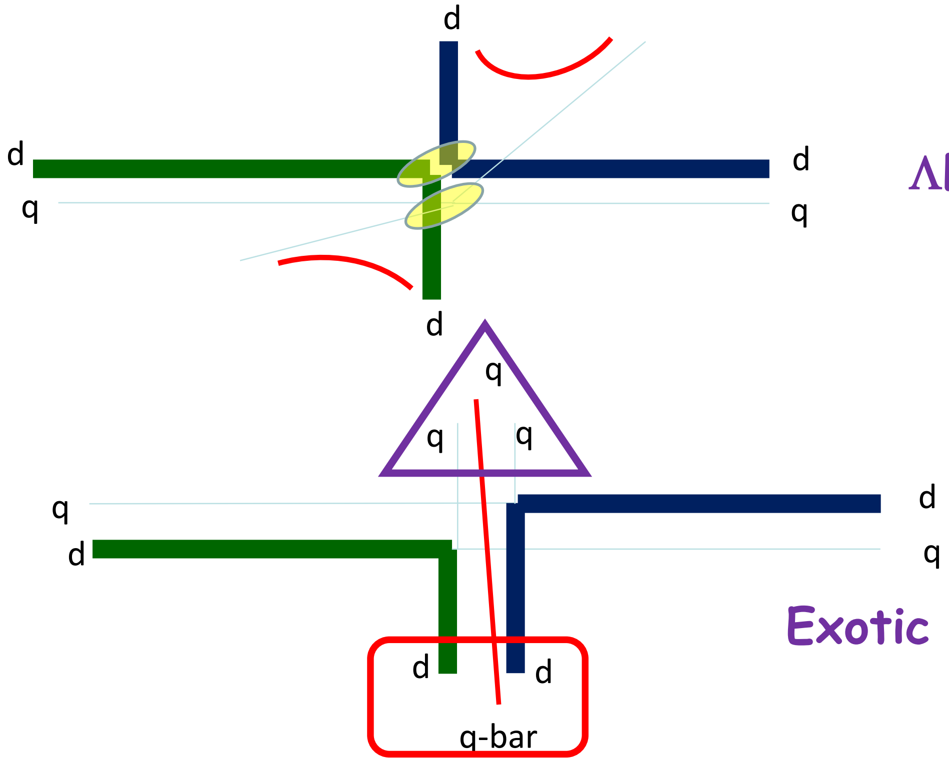

ΛK - interaction

Exotic states production

$\bar{p}p$ - reactions with tetraquarks production in

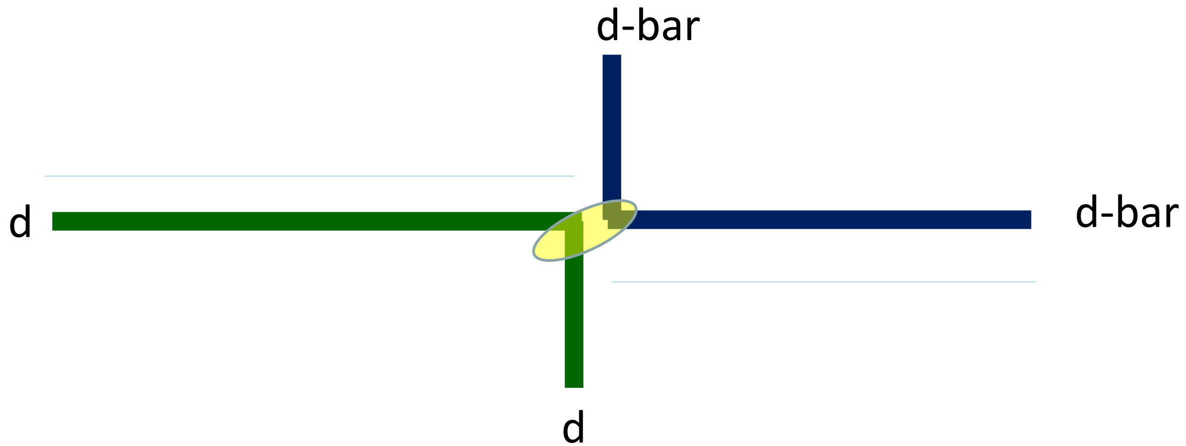

Diquark proof

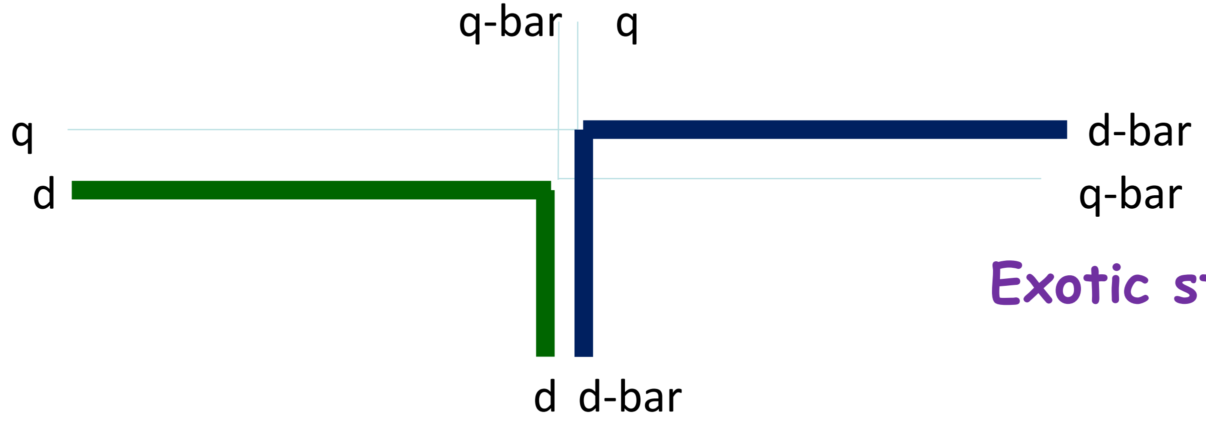

Exotic states production

Kim's-bar mechanisms

$\bar{p}d$ - reaction with tetraquarks +pentaquark production

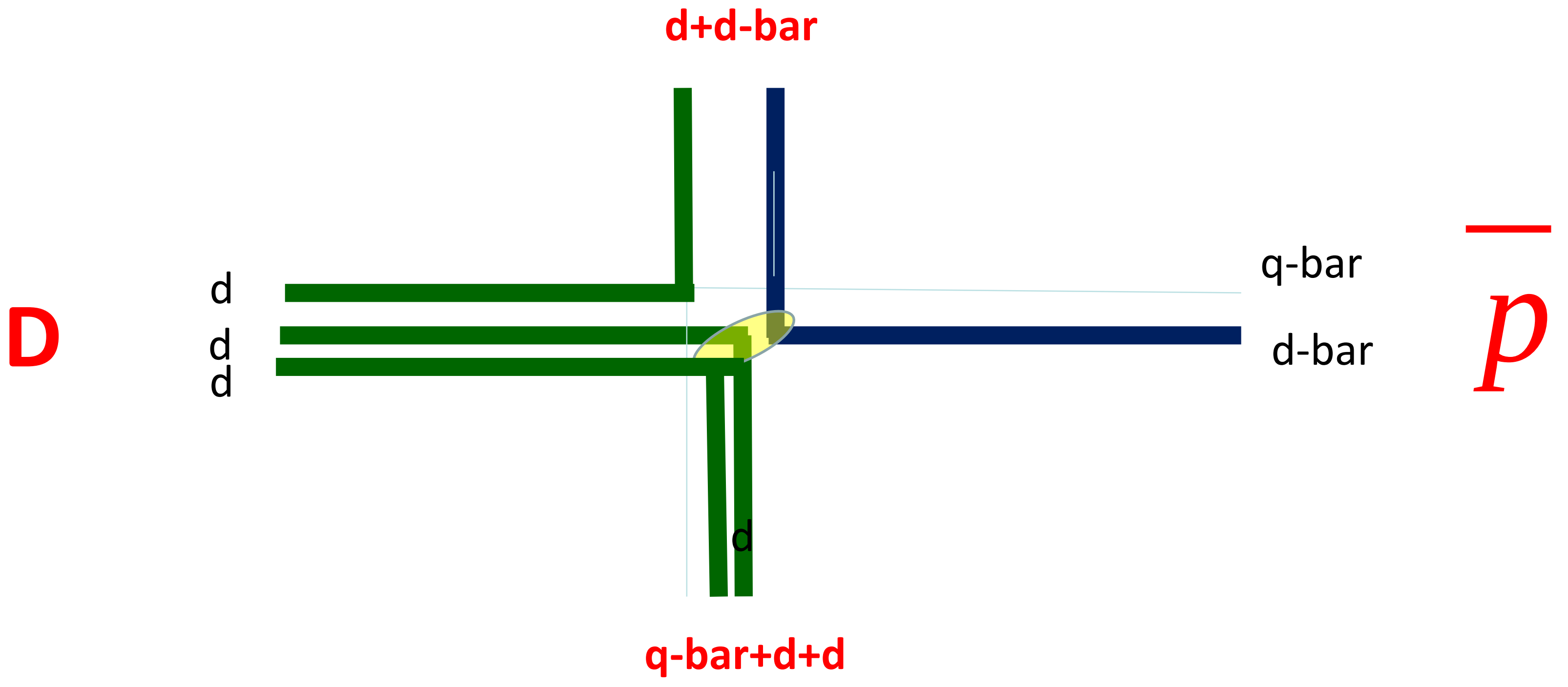

SPD Hybrid system

½ model symmetry

$B^{(z)}(x,y,0)=0.$

$J_T = 40\frac{A}{mm^2},$

$J^{(1,2)}_{B\backslash F} = \mp 80\frac{A}{mm^2},$

$S = 200\times 20\,mm^2,$

$I_T = J_T\cdot S = 160\,kA,$

$I_{B\backslash F} = J_{B\backslash F}\cdot S = \mp 320\,kA.$

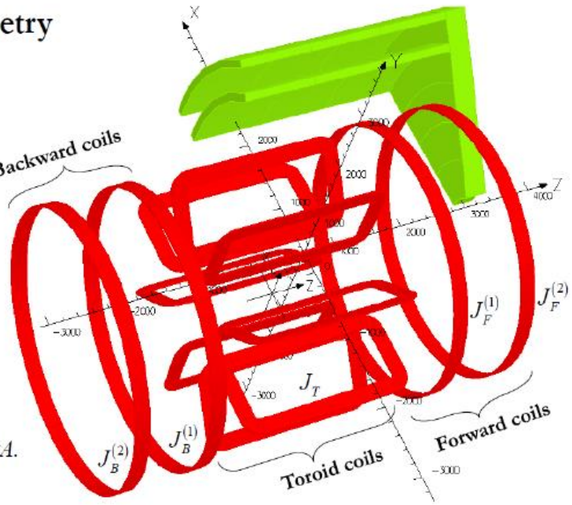

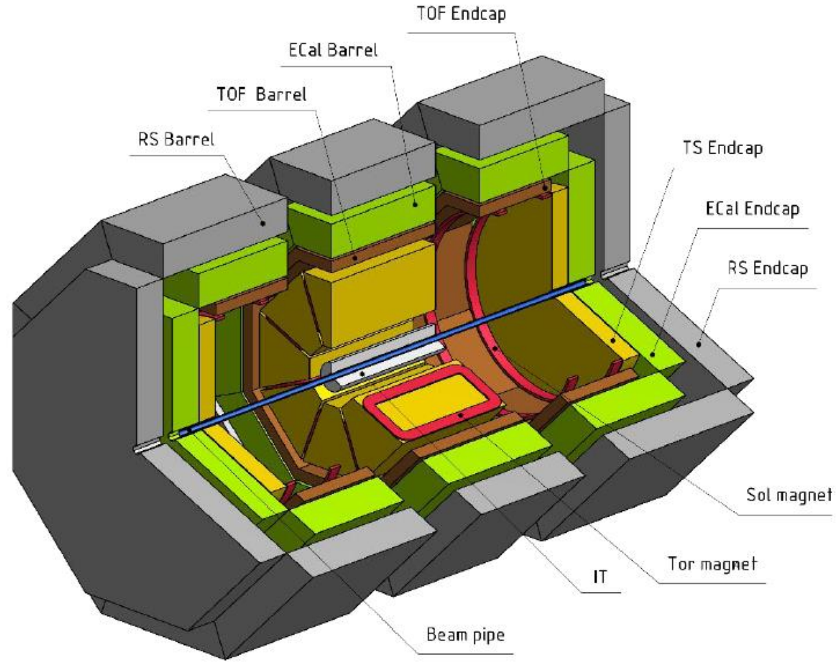

$\Omega = \left\{(r,\varphi,z):\ \begin{matrix}0\le r\le 3000\\ \varphi=0\\ 0\le z\le 3400\end{matrix}\right\}$

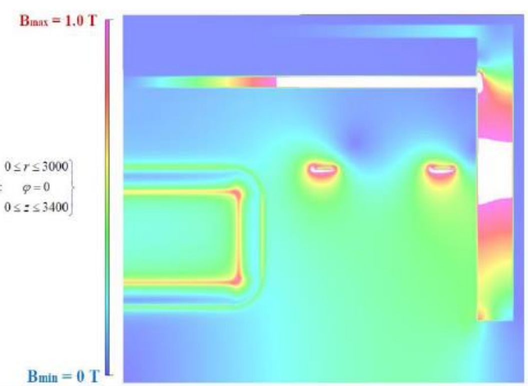

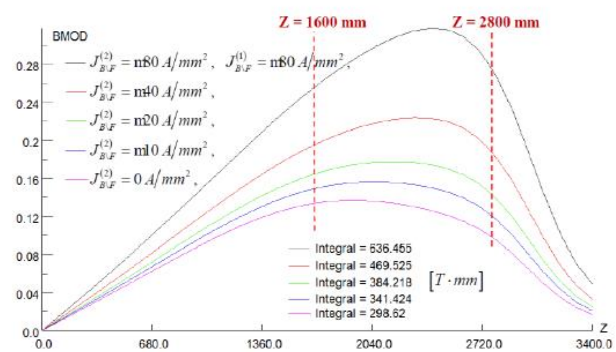

NICA Collision place for SPIN physics (deuteron and other beams, the first time all isotope states for NN system: pp, pn,nn.)

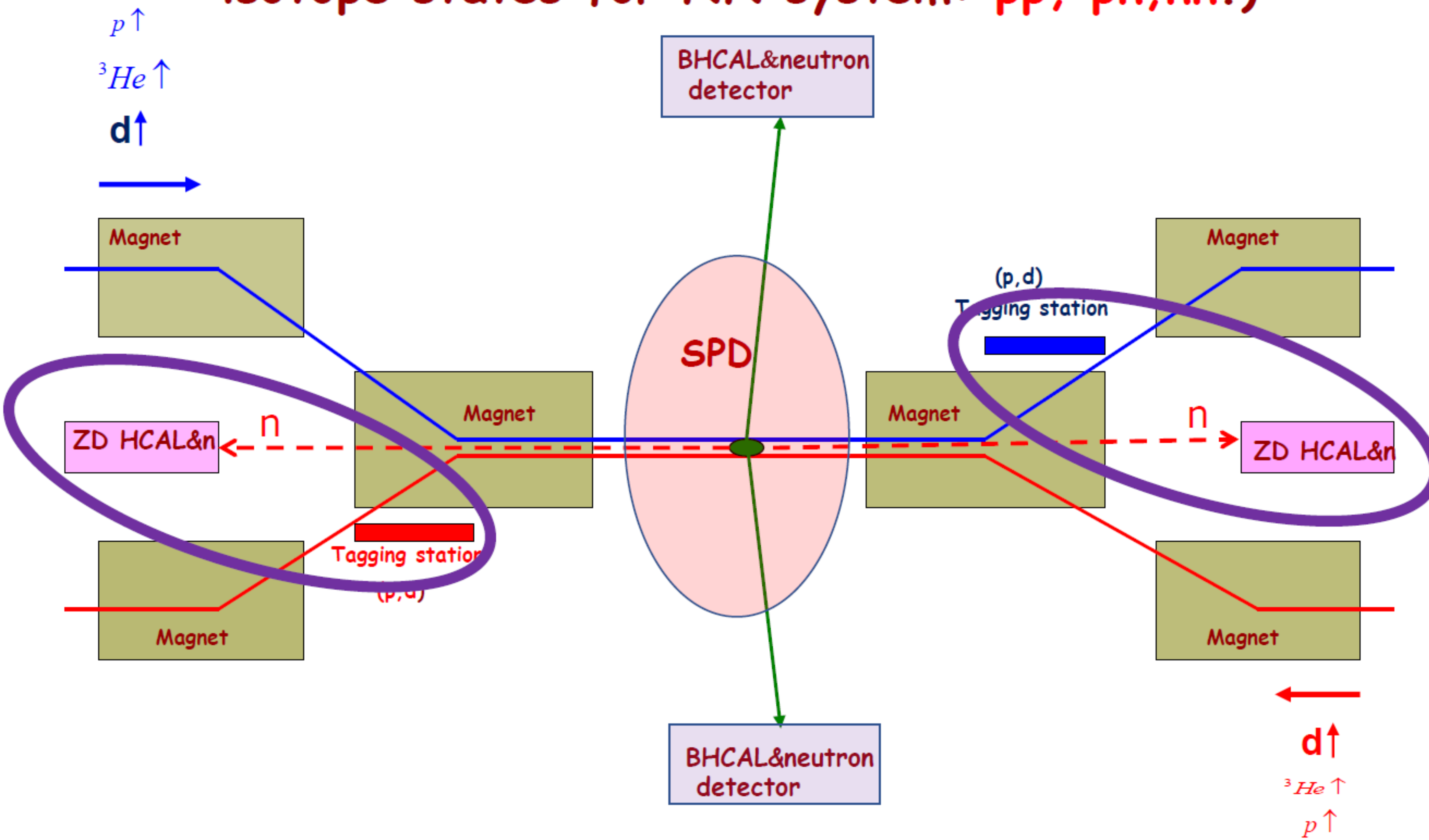

The tagging stations can be used as polarimeter!

END